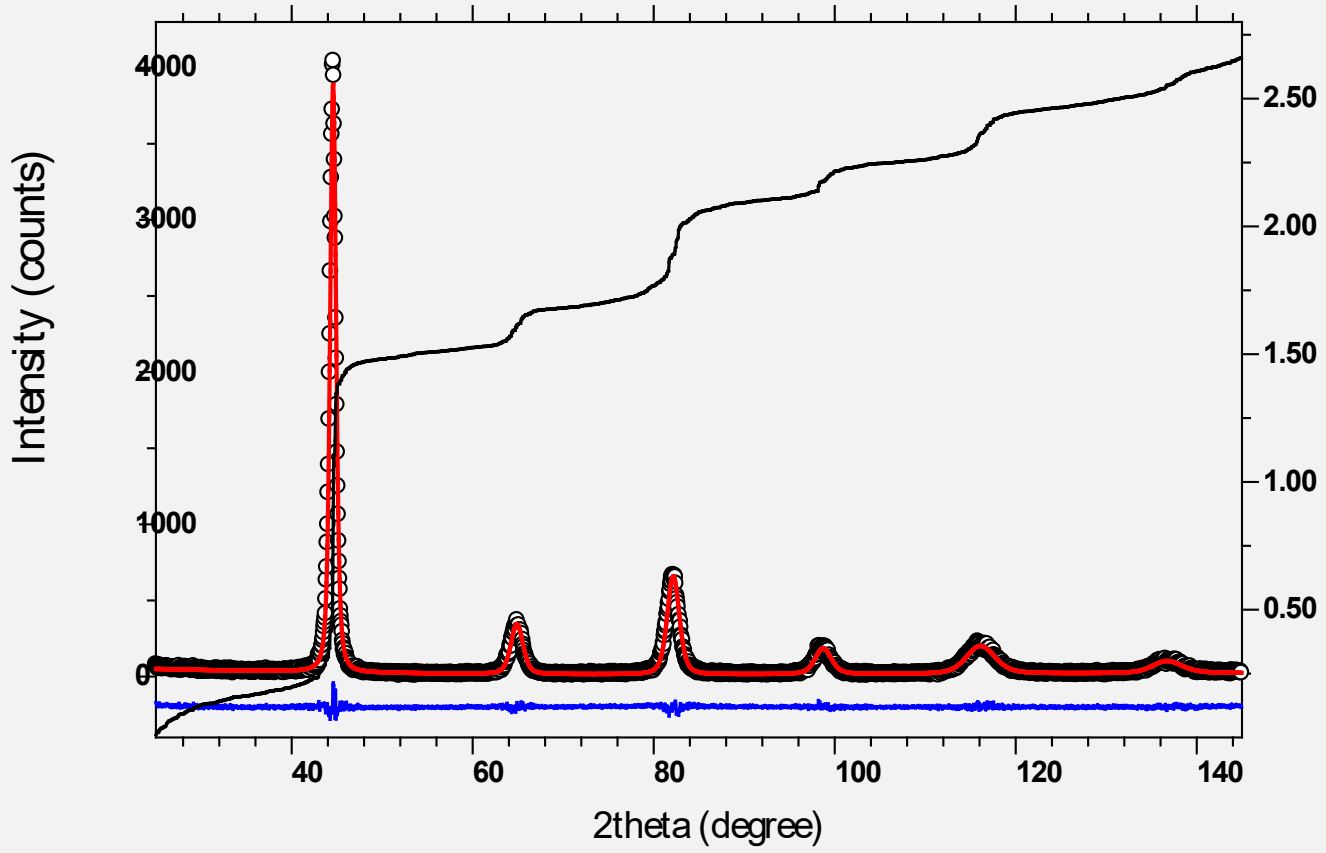


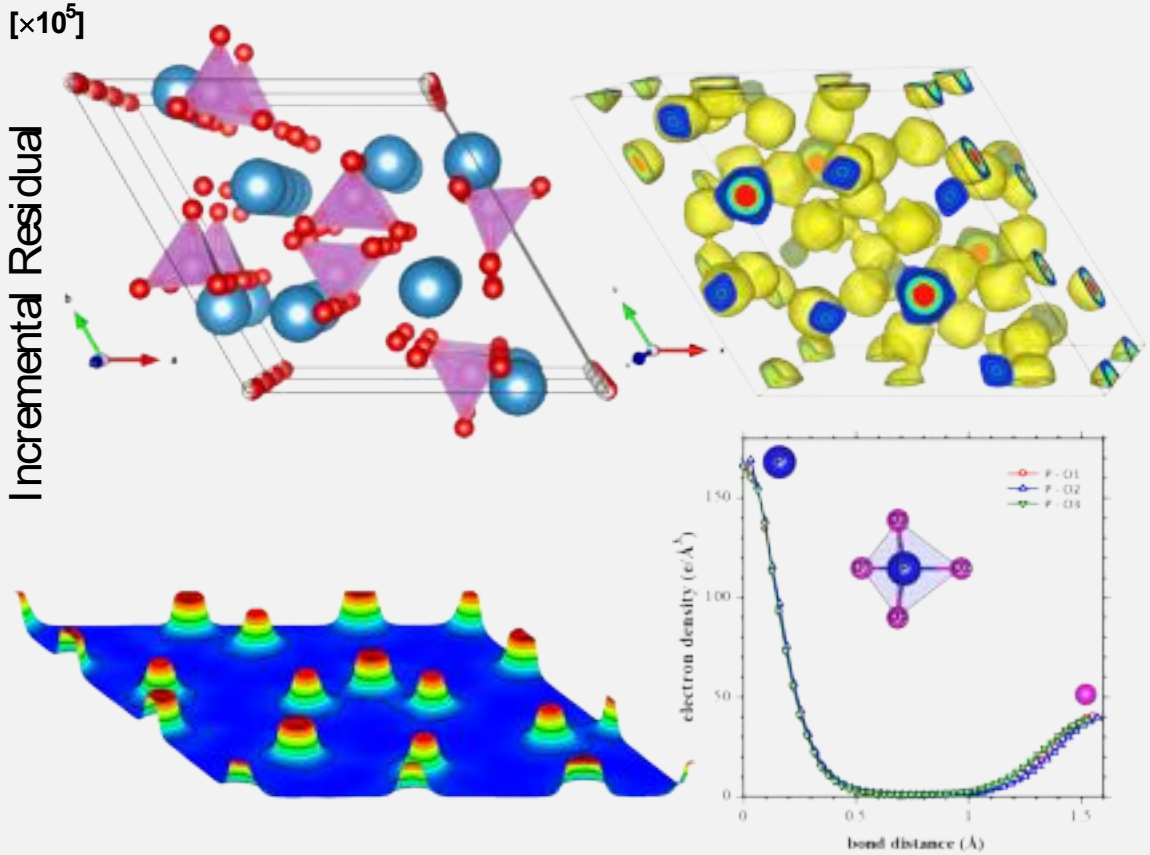


# Visualizing / Assessing ion-conduction pathway using Powder Diffraction

*Dr. Maykel T. E. Manawan //*

BRIN
BADAN RISET
DAN INOVASI NASIONAL

Queensland University of Technology

Australian Government
ANSTO

ICDD

# How does PXRD work?

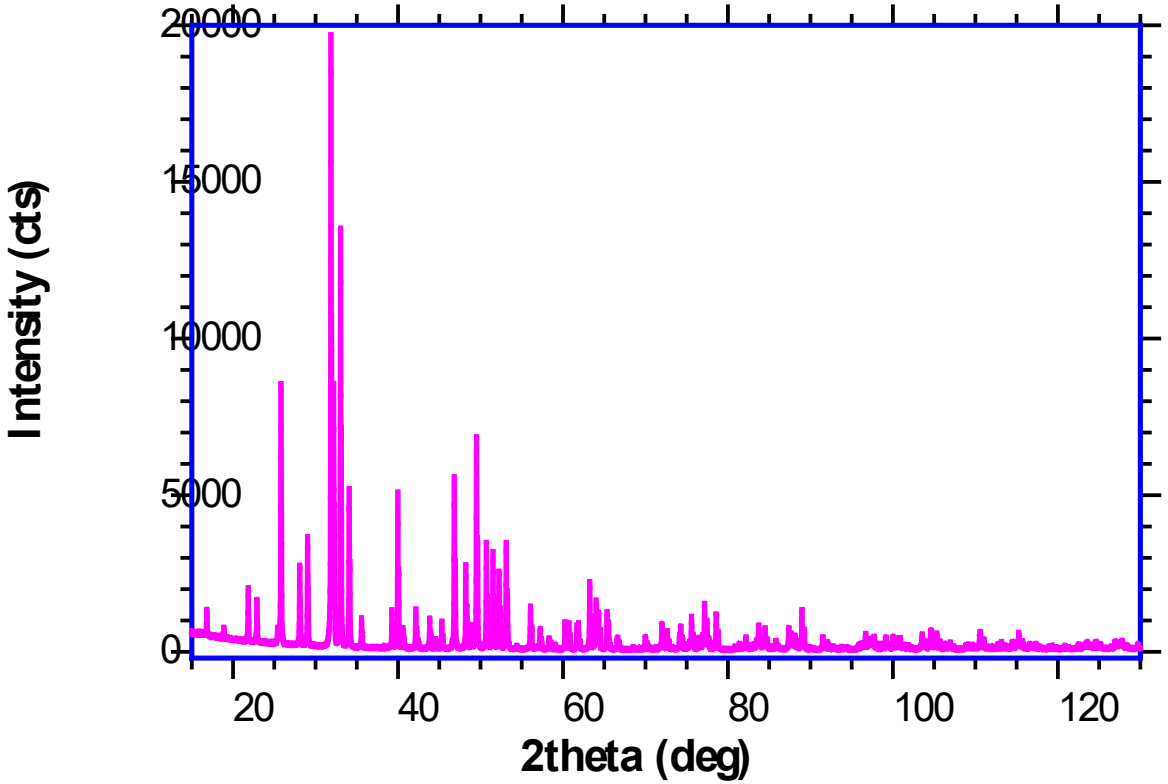


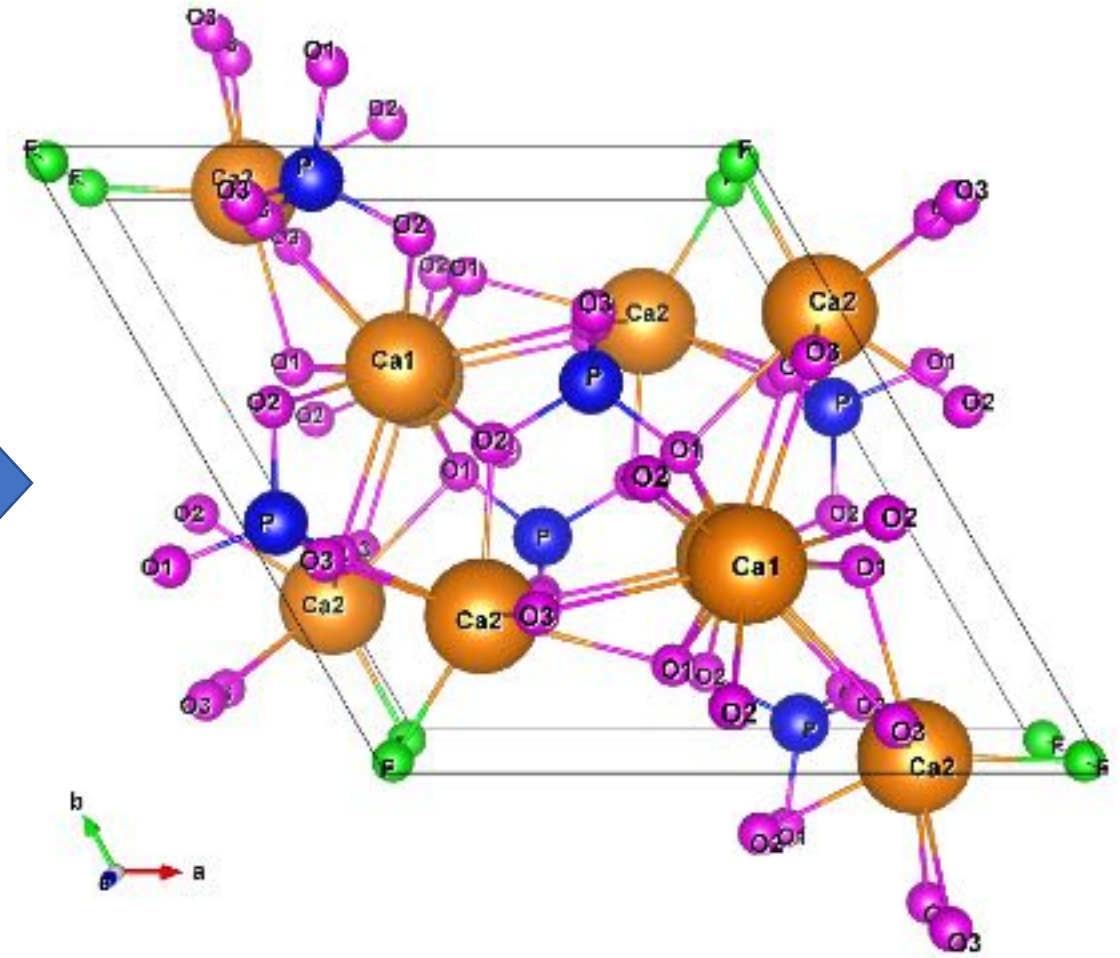

# The Structure & Fourier Transform

X-Ray

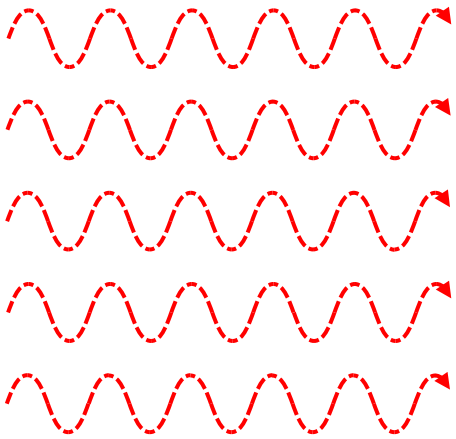

Crystal Space (3D)

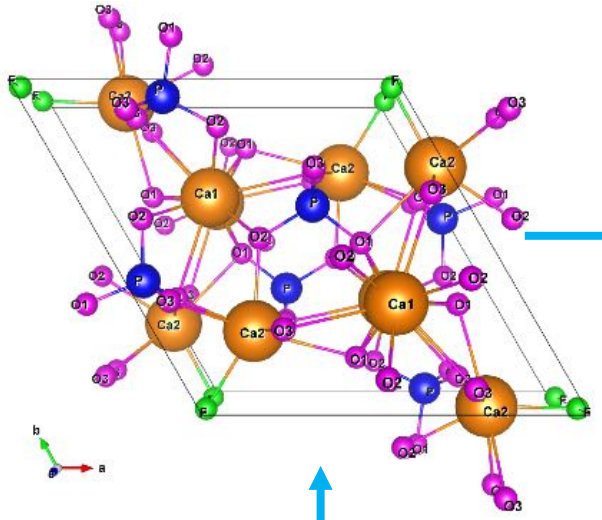


Reciprocal Space (1D)

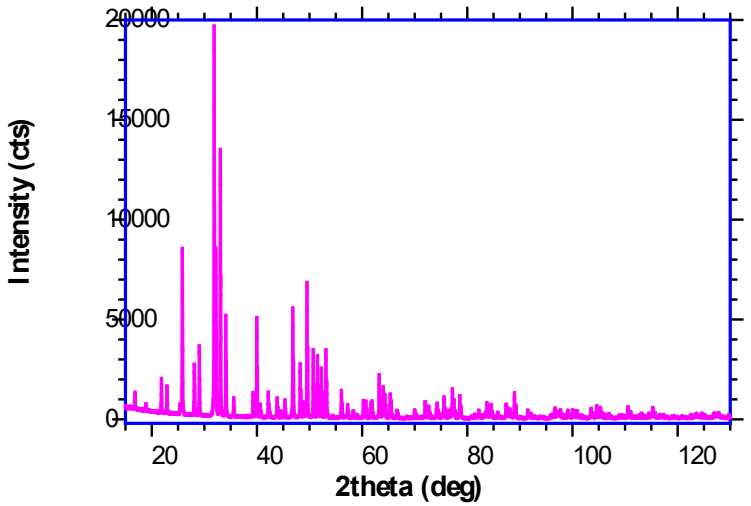


$I \sim F^2$

$$F_{hkl} = \sum_{1}^{N} f_n \, e^{2\pi i(hx_n + ky_n + lz_n)}$$

Fourier Synthesis

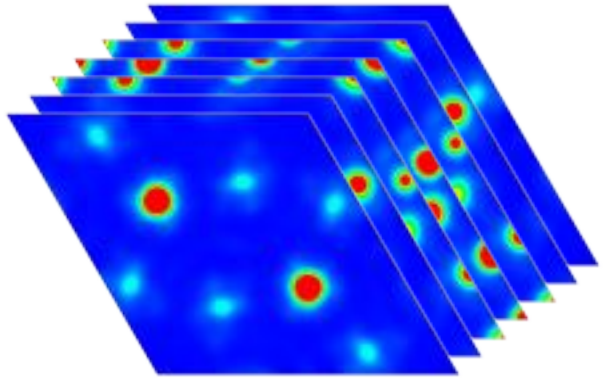

Electron/nuclear density map

# XRD Data Analysis Flow Chart

XRD (Emission, Radius, Optics, Detector)

RAW data (.brml, .raw, .xy)

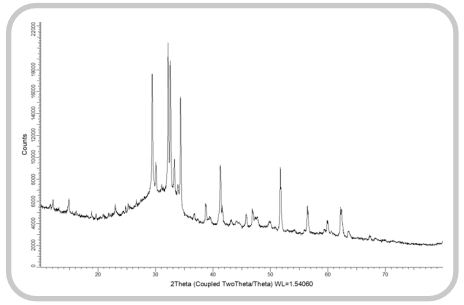

EVA

Qualitative Analysis (Search and Match)

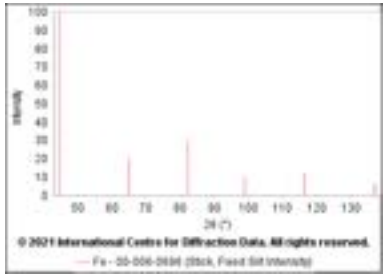

Stick pattern

ICDD-PDF4 (Database)

TOPAS

Quantitative Analysis (Rietveld analysis)

*.CIF, *.STR

Refinement report
- Diffractogram
- R-factors
- Structure
- QPA
- Crystallite Size
- Preferred Orientation
- etc.

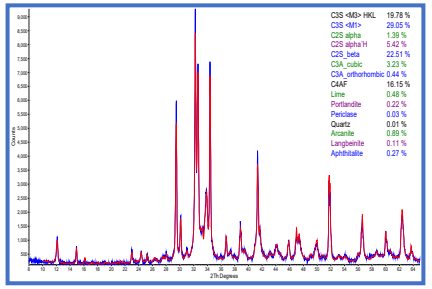

Refined Structure files
- *.CIF
- *.STR

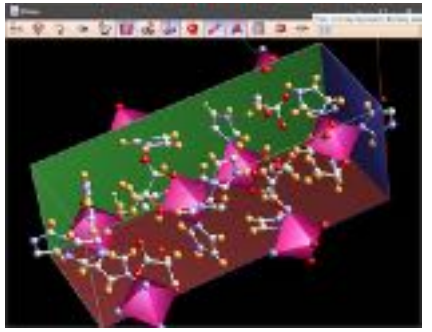

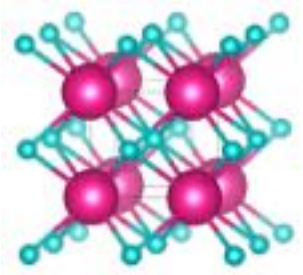

VESTA

# The Diffraction Intensity

$$I_k = SM_k L_k |F_k|^2 P_k A_k E_k$$

- ***S*** is an arbitrary scale factor,
  - used to adjust the relative contribution of individual phases to the overall diffraction pattern
- ***M*** is the multiplicity of the reflection
  - accounts for the fact that some observed diffraction peaks are actually the product of multiple equivalent planes diffracting at the same 2theta; example: (001) (100) (010) etc in cubic
  - automatically calculated based on the crystal structure
- ***L*** is the Lorentz polarization factor
- ***F*** is structure factor, which is the amplitude of scattered light due to the crystal structure
- ***P*** is the modification of intensity due to preferred orientation
- ***A*** is absorption correction
- ***E*** is extinction correction

# Structure factor

$$F_{hkl} = \sum_{1}^{N} f_n \, e^{2\pi i(hx_n + ky_n + lz_n)}$$

$$F_{hkl} = \sum_{1}^{N} f_n \left[\cos 2\pi(hx_n + ky_n + lz_n) + i \sin 2\pi(hx_n + ky_n + lz_n)\right]$$

$$F^2 = \left[f_1 \cos 2\pi(hx_1 + ky_1 + lz_1) + f_2 \cos 2\pi(hx_2 + ky_2 + lz_2) + \cdots\right]^2 + \left[f_1 \sin 2\pi(hx_1 + ky_1 + lz_1) + f_2 \sin 2\pi(hx_2 + ky_2 + lz_2) + \cdots\right]^2$$

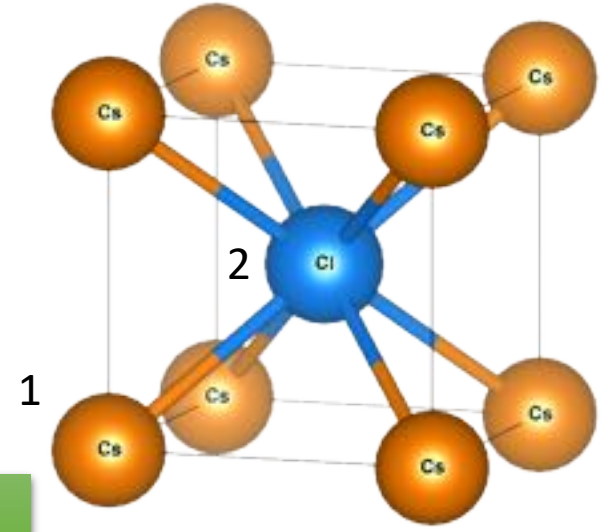


- The structure factor quantifies the amplitude of X-rays scattered by a crystal
- $F_{hkl}$ sums the result of scattering from all of the atoms in the unit cell to form a diffraction peak from the (*hkl*) planes of atoms
- The amplitude of scattered light is determined by:
  - where the atoms are on the (*hkl*) planes
    - this is expressed by the fractional coordinates $x_n$ ,$y_n$,$z_n$
  - what atoms are on the atomic planes
    - the scattering factor $f_n$ quantifies the relative efficiency of scattering at any angle by the group of electrons in each atom

# Atomic scattering factor

$$|f|^2 = \left( f_0 \exp\left[ -\frac{B \sin^2 \theta}{\lambda^2} \right] + (\Delta f')^2 \right)^2 + (\Delta f'')^2$$

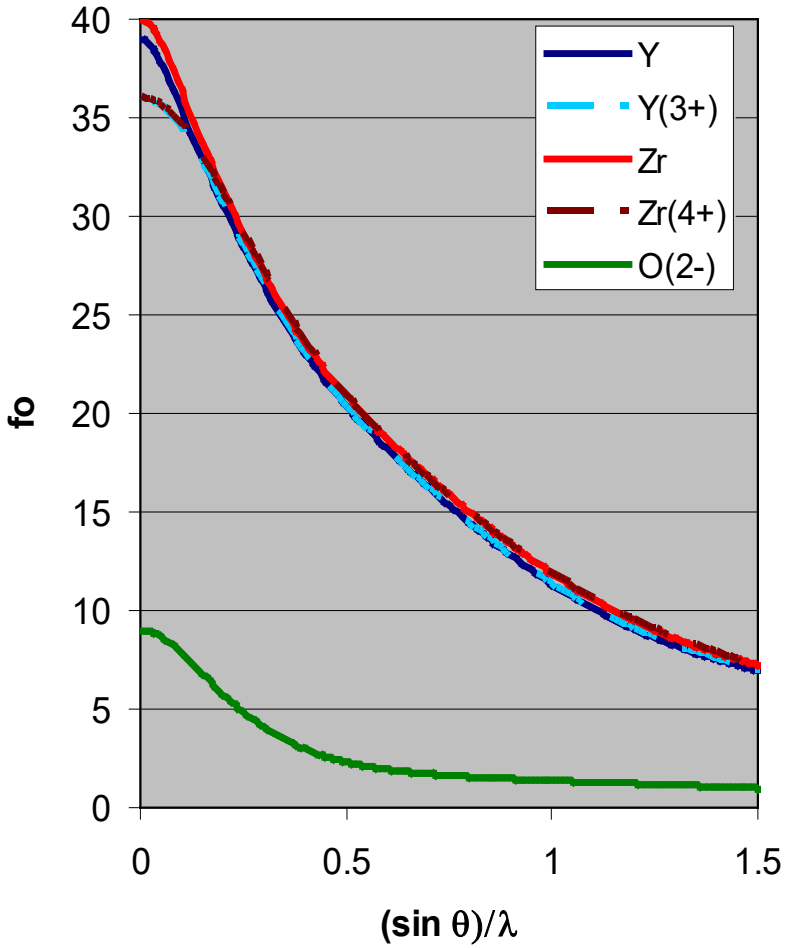


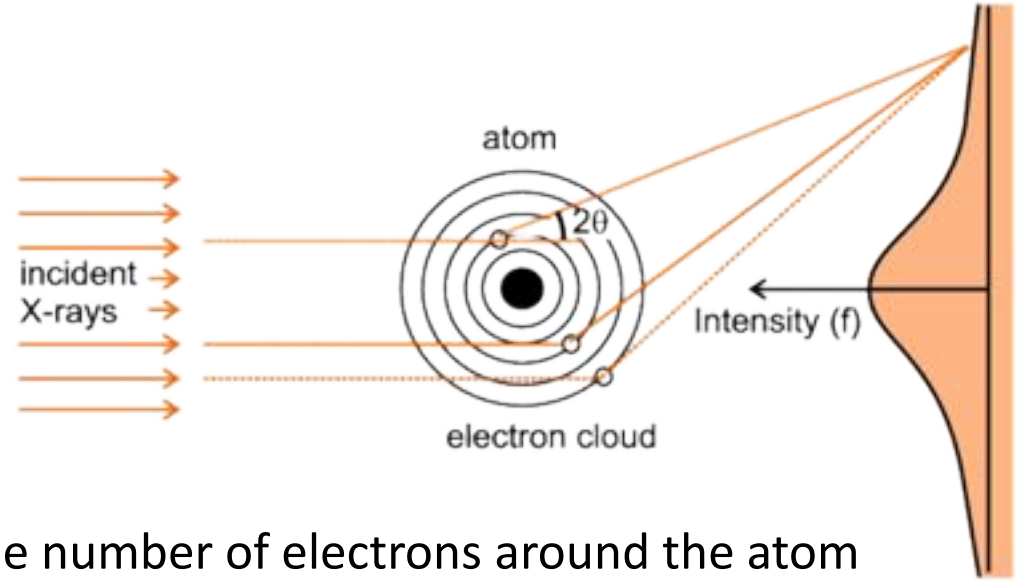


- $f_0$ at 0° is equal to the number of electrons around the atom
  - Y and Zr are similar, but slightly different, at 0°
  - Zr and $Zr^{4+}$ are slightly different at 0°
  - $Y^{3+}$ and $Zr^{4+}$ are identical at 0°
- The variation with (sin θ)/λ depends on size of atom
  - smaller atoms drop off quicker
  - at higher angles, the difference between $Y^{3+}$ and $Zr^{4+}$ is more readily discerned
  - at higher angles, the difference between different oxidation states (eg Zr and $Zr^{4+}$) is less prominent

# Temperature Factor

$$f = f_0 \exp\left[-\frac{B \sin^2 \theta}{\lambda^2}\right]$$

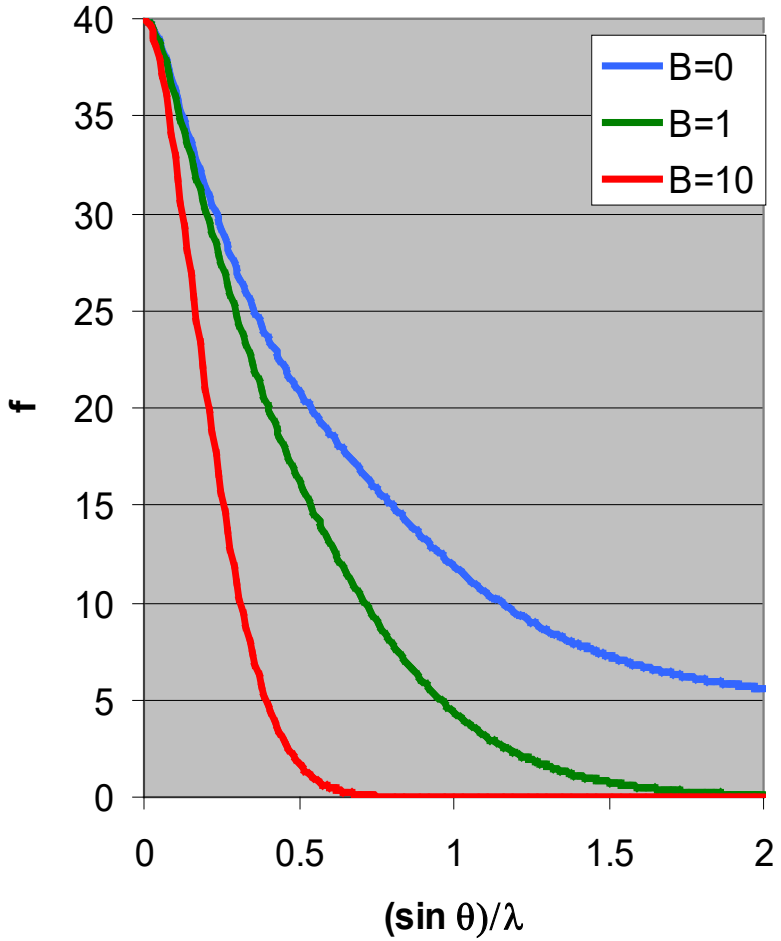


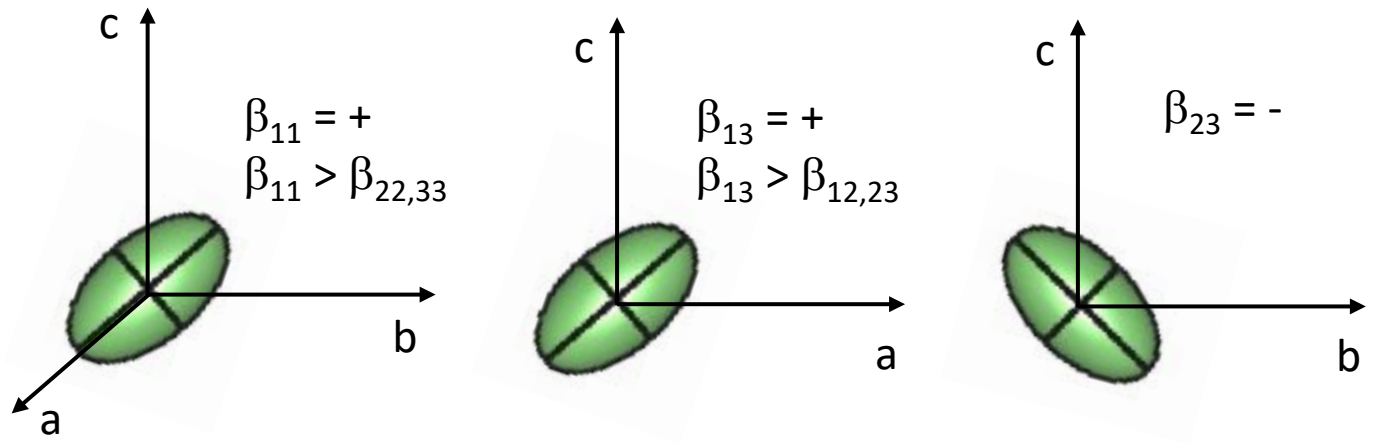


- Efficiency of scattering by an atom is reduced because the atom and its electrons are not stationary - atom is vibrating about its equilibrium lattice site
- The amount of vibration is quantified by the Debye-Waller temperature factor:
  - $B=8\pi^2u^2$, $u^2$ is the mean-square amplitude of the vibration
  - this is for isotropic vibration: sometimes B is broken down into six $B_{ij}$ anisotropic terms if the amplitude of vibration is not the same in all directions.
  - aka temperature factor, displacement factor, thermal displacement parameter

# What is MEM and what it does?

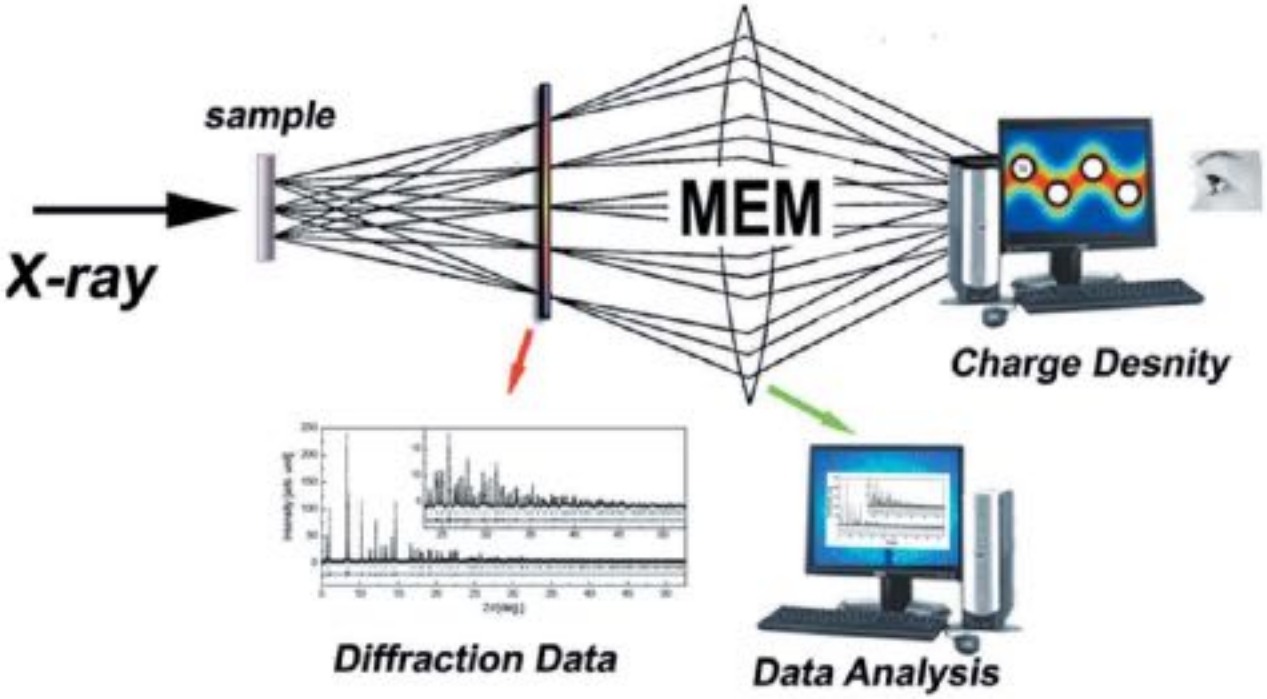


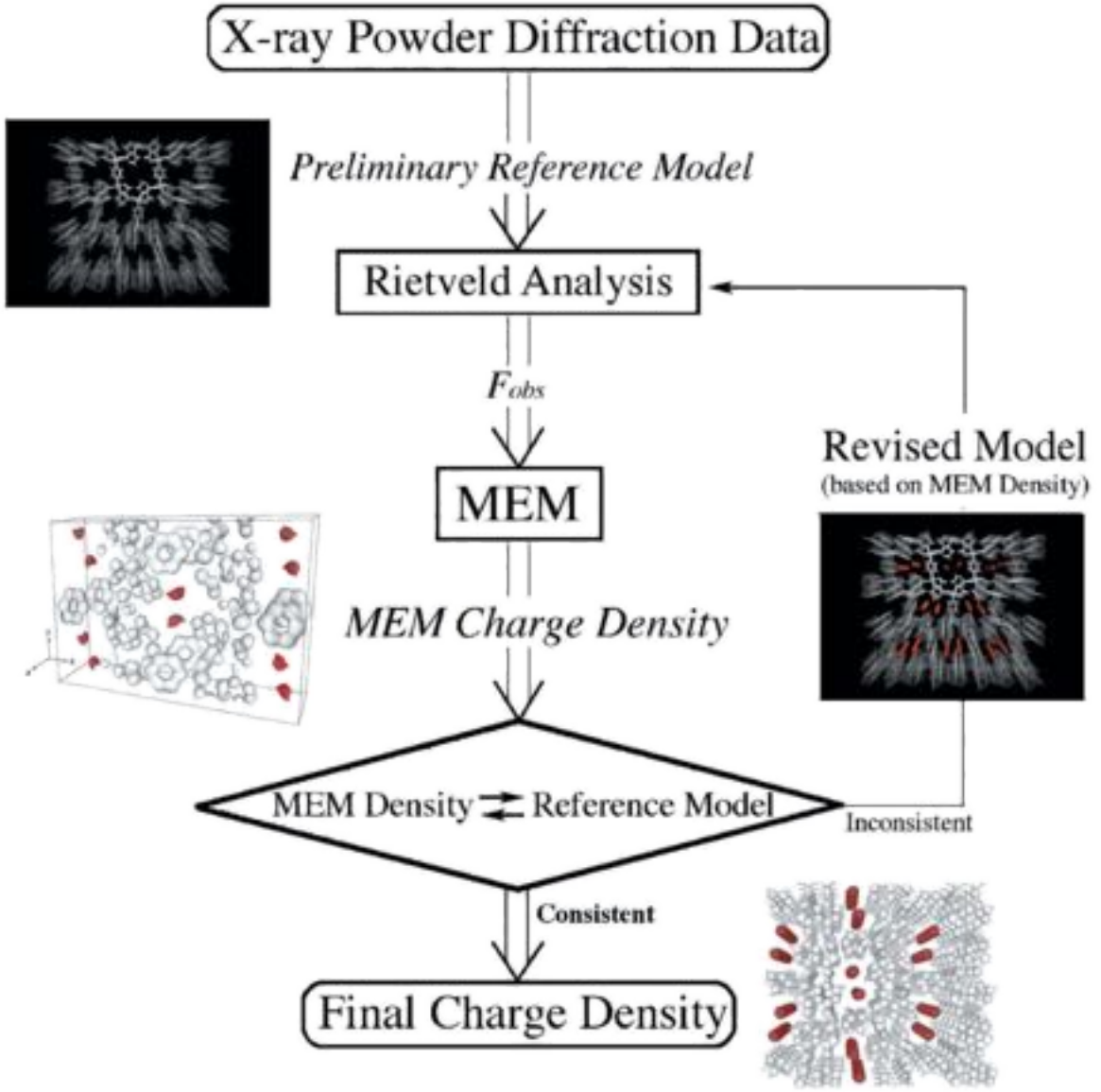


*International Tables for Crystallography* (2019). Vol. H, Chapter 4.8, pp. 473–488.

# What is MEM and what it does? (Cont.)

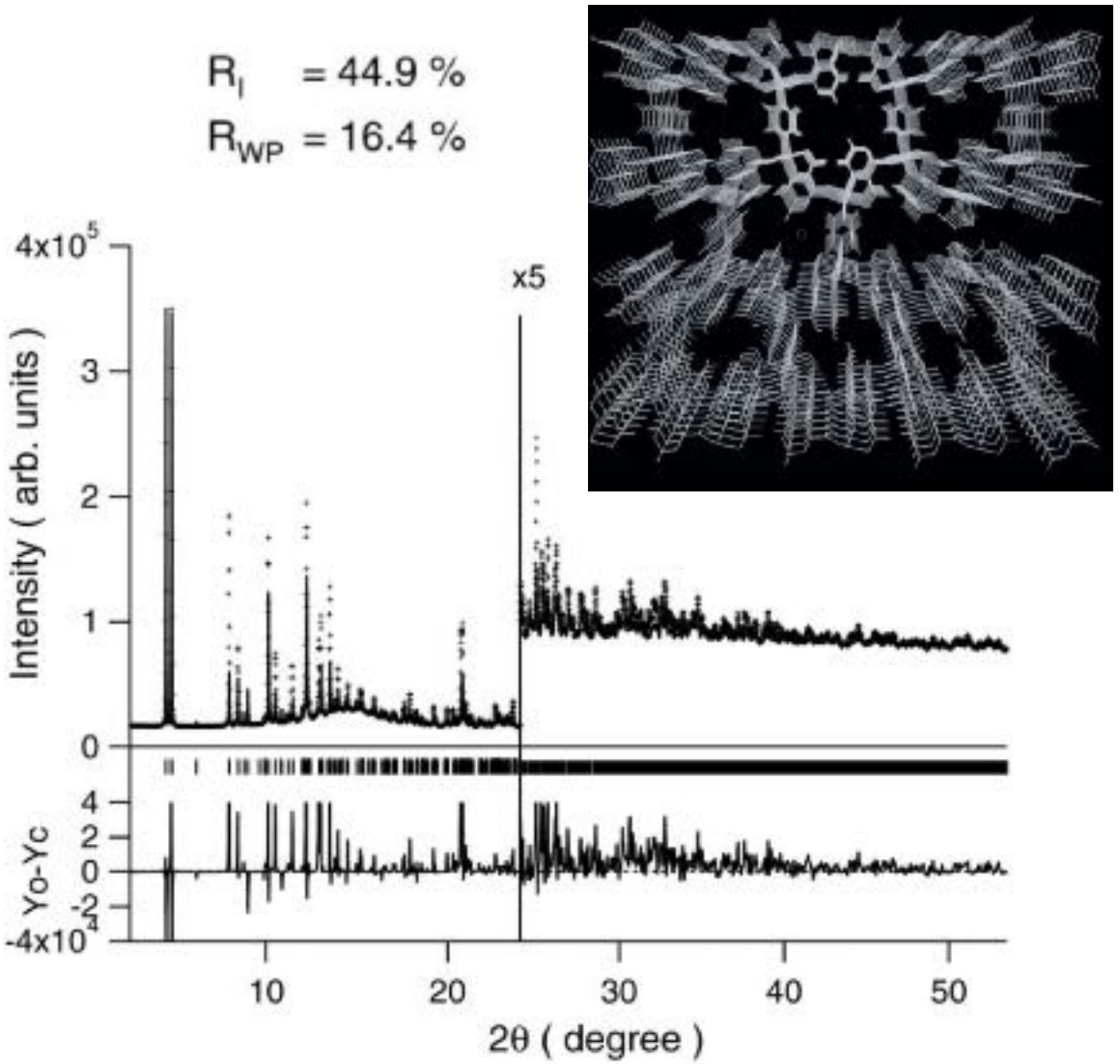


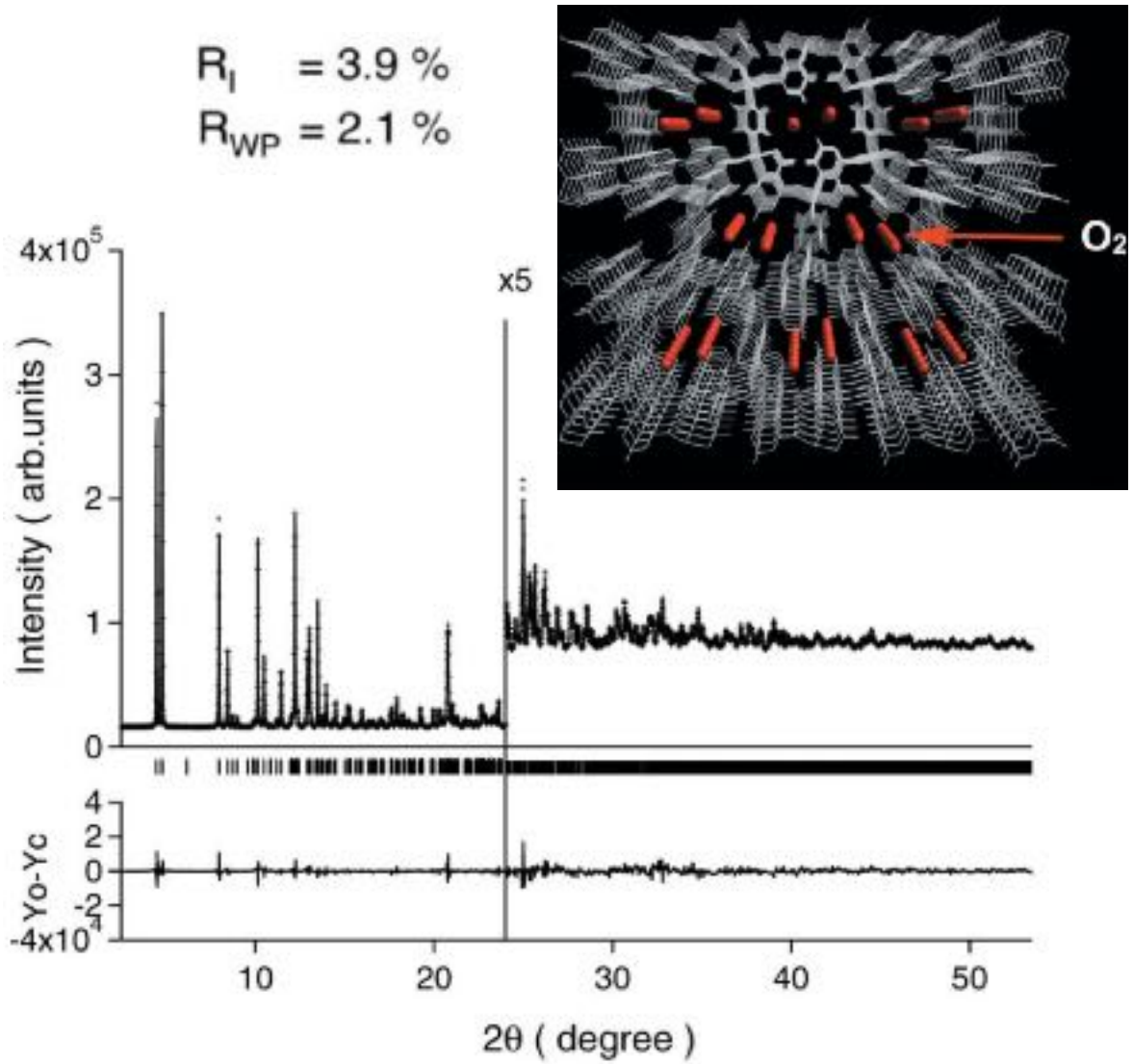


*International Tables for Crystallography* (2019). Vol. H, Chapter 4.8, pp. 473–488.

# MEM Basic Principle

Collins's formalism is based on the entropy expression, $S$, obtained by Jaynes (1968):

$$S = -\sum_{\mathbf{r}} \rho'(\mathbf{r}) \ln [\rho'(\mathbf{r})/\tau'(\mathbf{r})]. \quad (1)$$

The probability $\rho'(\mathbf{r})$ and prior probability $\tau'(\mathbf{r})$ are connected with the actual electron density by

$$\rho'(\mathbf{r}) = \rho(\mathbf{r})/\sum_{\mathbf{r}} \rho(\mathbf{r}) \quad (2)$$

$$\tau'(\mathbf{r}) = \tau(\mathbf{r})/\sum \tau(\mathbf{r}) \quad (3)$$

where $\rho(\mathbf{r})$ is the electron density at a certain pixel $\mathbf{r}$ and $\tau(\mathbf{r})$ is the prior density for $\rho(\mathbf{r})$.

We introduce two types of weak constraints as given information; one is for phase-known structure factors and the other is for phase-unknown structure factors.

$$C_1 = (1/N_1) \sum_{\mathbf{k}} |F_{\text{cal}}(\mathbf{k}) - F_{\text{obs}}(\mathbf{k})|^2/\sigma^2(\mathbf{k}) \quad (4)$$

$$C_2 = (1/N_2) \sum_{\mathbf{k}} ||F_{\text{cal}}(\mathbf{k})| - |F_{\text{obs}}(\mathbf{k})||^2/\sigma^2(\mathbf{k}) \quad (5)$$

where $N_1$ and $N_2$ are the number of reflections for phase-known and phase-unknown structure factors, respectively, $F_{\text{obs}}(\mathbf{k})$ is the observed structure factor for reflection $\mathbf{k}$, $\sigma(\mathbf{k})$ the standard deviation of $F_{\text{obs}}(\mathbf{k})$, and $F_{\text{cal}}(\mathbf{k})$ is the calculated structure factor given as

$$F_{\text{cal}}(\mathbf{k}) = V \sum_{\mathbf{r}} \rho(\mathbf{r}) \exp(-2\pi i \mathbf{r} \cdot \mathbf{k}), \quad (6)$$

where $V$ is the unit-cell volume. The expected value for $C_1$ and $C_2$ is 1. The sums in (4) and (5) are taken over the set of points for which the phase-known and phase-unknown structure-factor data are measured.

We use Lagrange's method of undetermined multipliers to constrain $C_1$ to be unity while we maximize the entropy. Then we have

$$Q(\lambda_1, \lambda_2) = -\sum_{\mathbf{r}} \rho(\mathbf{r}) \ln [\rho(\mathbf{r})/\tau(\mathbf{r})] - (\lambda_1/2)C_1 - (\lambda_2/2)C_2, \quad (7)$$

where $\lambda_1$ and $\lambda_2$ are Lagrange multipliers. By setting

$$\partial Q(\lambda_1, \lambda_2)/\partial \rho(\mathbf{r}) = 0 \quad (8)$$

and using some approximations given by Collins (1982), we have

$$\begin{aligned}\rho(\mathbf{r}) = \exp [&\ln \tau(\mathbf{r}) + (\Lambda_1/N_1) \sum [1/\sigma^2(\mathbf{k})] \\ &\times \{F_{\text{obs}}(\mathbf{k}) - F_{\text{cal}}(\mathbf{k})\} \exp(-2\pi i \mathbf{k} \cdot \mathbf{r}) \\ &+ (\Lambda_2/N_2) \sum [1/\sigma^2(\mathbf{k})] \\ &\times \{|F_{\text{obs}}(\mathbf{k})| \exp [i\varphi(\mathbf{k})] - F_{\text{cal}}(\mathbf{k})\} \\ &\times \exp(-2\pi i \mathbf{k} \cdot \mathbf{r})], \end{aligned} \quad (9)$$

where

$$\Lambda_1 = \lambda_1 F_0, \qquad \Lambda_2 = \lambda_2 F_2 \quad (10)$$

and $F_0$ is equal to the number of electrons in a unit cell, $Z$. In the present study, we strictly confine the total number of electrons in the unit cell to be $Z$. Since all the structure factors are known on an absolute scale, this can be done in a straightforward way. When $F_{\text{obs}}(\mathbf{k})$, $\sigma(\mathbf{k})$ and $\lambda_i$ are given, we can obtain (9) which determines the MEM estimate for the electron-density distribution, $\rho_{\text{MEM}}(\mathbf{r})$. In practice, the value of $\rho_{\text{MEM}}(\mathbf{r})$ has been solved numerically by an iterative procedure, starting from the uniform electron density.

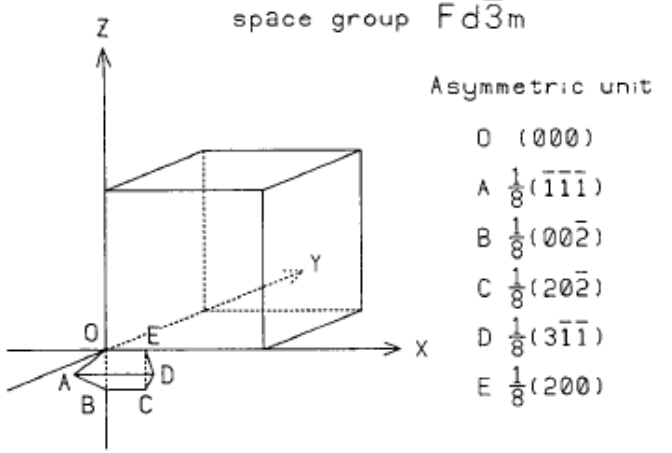


Fig. 1. Unit cell and asymmetric unit of space group $Fd\bar{3}m$.

In the present work, we use our knowledge of the space group. For this purpose, we calculate the electron density in the region of the minimum asymmetric unit. In the case of Si, of which the space group is $Fd\bar{3}m$, the asymmetric unit is written as $0 \le x \le \frac{1}{2}$; $0 \le y \le \frac{1}{8}$; $-\frac{1}{8} \le z \le \frac{1}{8}$; $y \le \min(\frac{1}{2} - x, x)$; $-y \le z \le y$ (*International Tables for Crystallography*, 1983). This asymmetric unit is shown in Fig. 1. After calculating the electron-density distribution of the minimum asymmetric unit by using (9), we can produce the electron-density distribution for the whole unit cell through the symmetry operations.

Sakata, M. & Sato, M. (1990) Acta Cryst. **A46**, 263-270

# MEM basic principle (cont.)

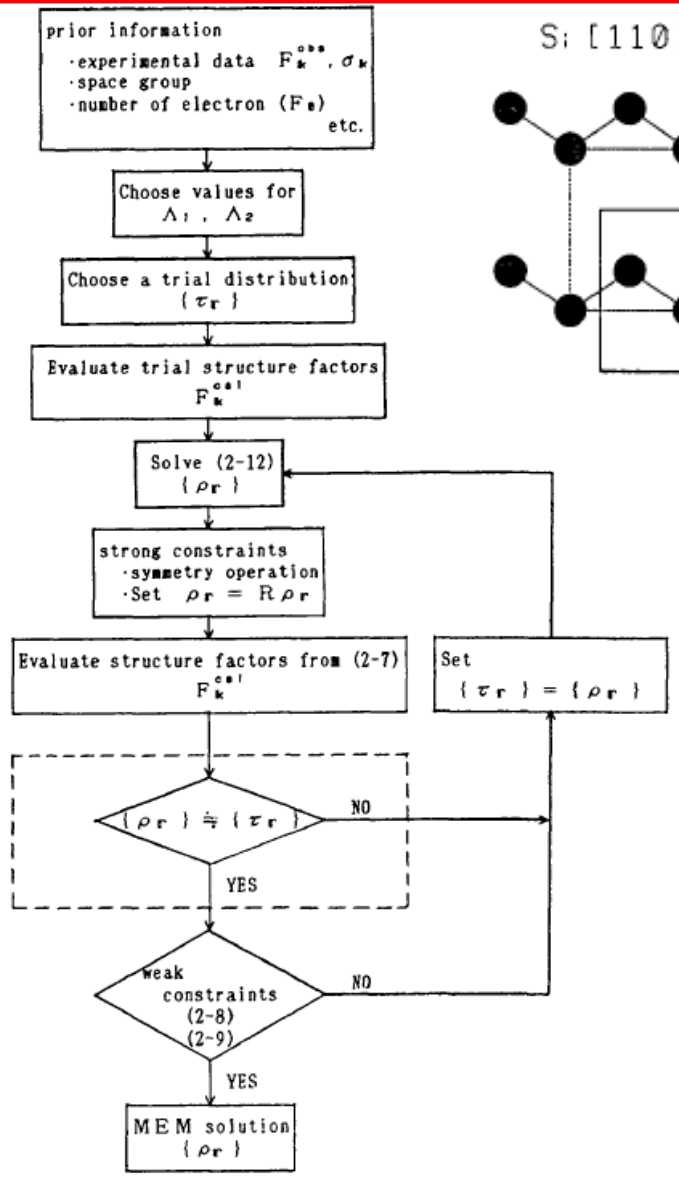


Fig. 2. Flow chart for the present calculation with the maximum-entropy method.

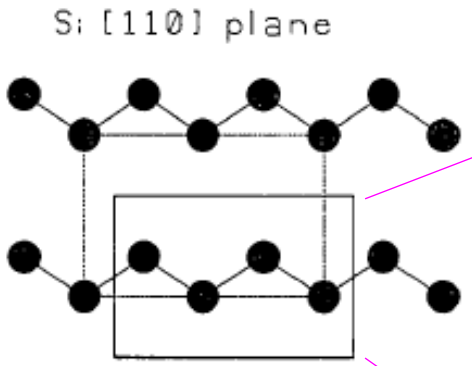


Direct Fourier Method

Maximum Entropy Method

High density region

Low density region

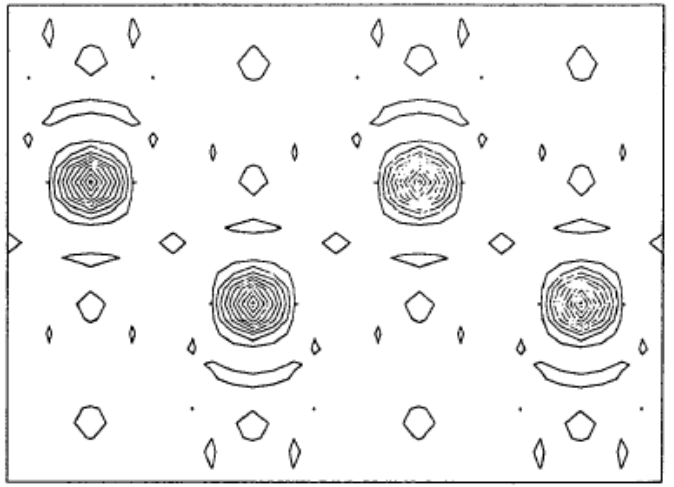

1.6 to 91.6 with 10.0 intervals (eÅ$^3$)

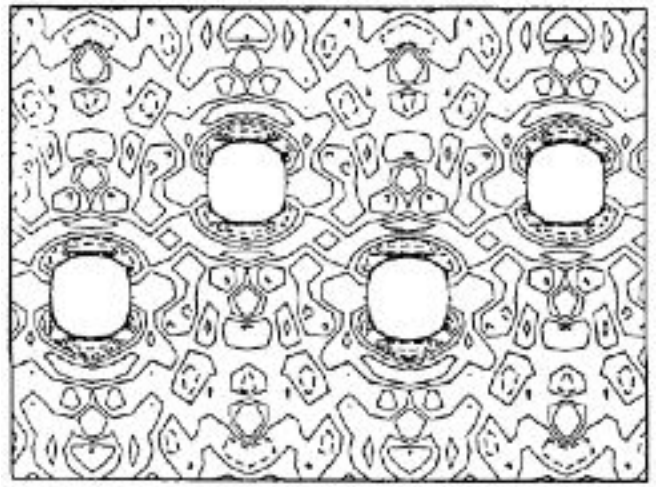

-2.40 to 1.6 with 0.8 intervals (eÅ$^3$)

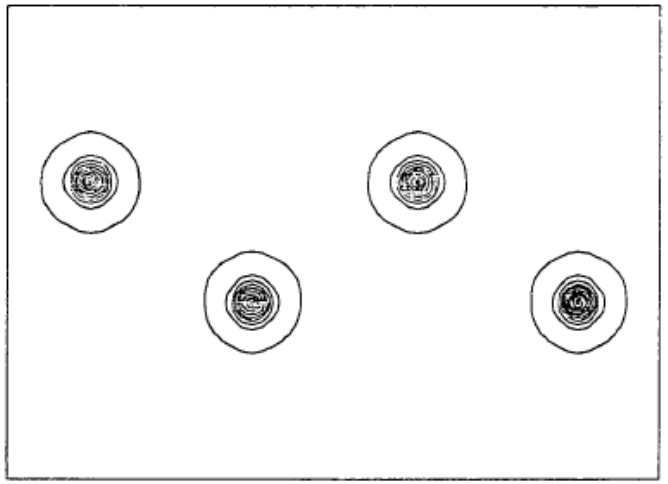

1.50 to 201.5 with 20.0 interval (eÅ$^3$)

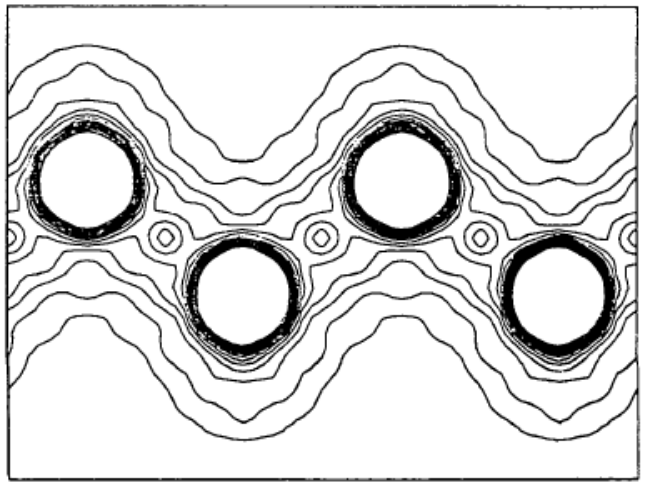

0.1 to 1.5 with 0.1 intervals (eÅ$^3$)

# MEM technology in Rietan-FP

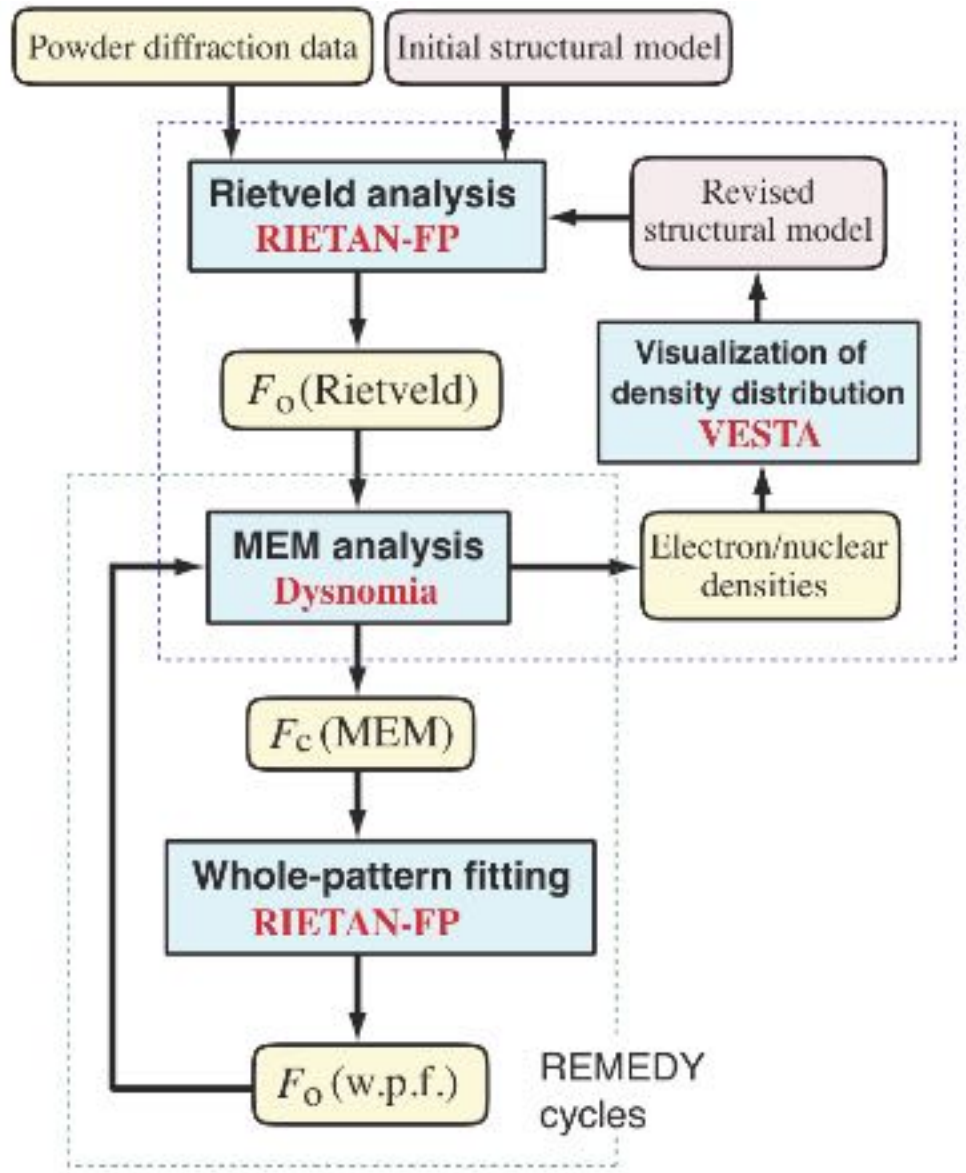


As Fig. 1 illustrates schematically, MPF (lower box) follows the MEM/Rietveld analyses (upper box). $F_c$(MEM)s can be calculated by the Fourier transform of 3D densities resulting from the MEM analysis. It is the $F_c$(MEM) data that minimize the bias toward the structural model. In each whole-pattern fitting (w.p.f.), we fit a calculated pattern to the observed one in the whole $2\theta$ range by fixing structure factors at the values of $F_c$(MEM) obtained in the previous MEM analysis and by refining only parameters irrelevant to the structure, e.g., scale factor, and profile, lattice, and background parameters. $F_o$(w.p.f.)s evaluated after w.p.f. according to Rietveld's procedure [2] are analyzed again by MEM. In this way, MEM analysis and w.p.f. are alternately repeated (REMEDY cycles) until $R$ factors (usually $R_{wp}$) in the latter no longer decrease.

Such an iterative procedure is somewhat similar to the Le Bail method [3] but differs from it in the point that structure factors in w.p.f. are fixed at $F_c$(MEM)s resulting from the previous MEM analysis. REMEDY cycles weaken the influence of the structural model on $F_o$(w.p.f.)s. In other words, intensity repartitioning for overlapping reflections becomes more appropriate with the increasing number of cycles owing to extraction of additional structural information from observed intensities of Bragg reflections.

Izumi, F. (2004) Solid State Ionics **172**, 1 –6

# What are the Differences?

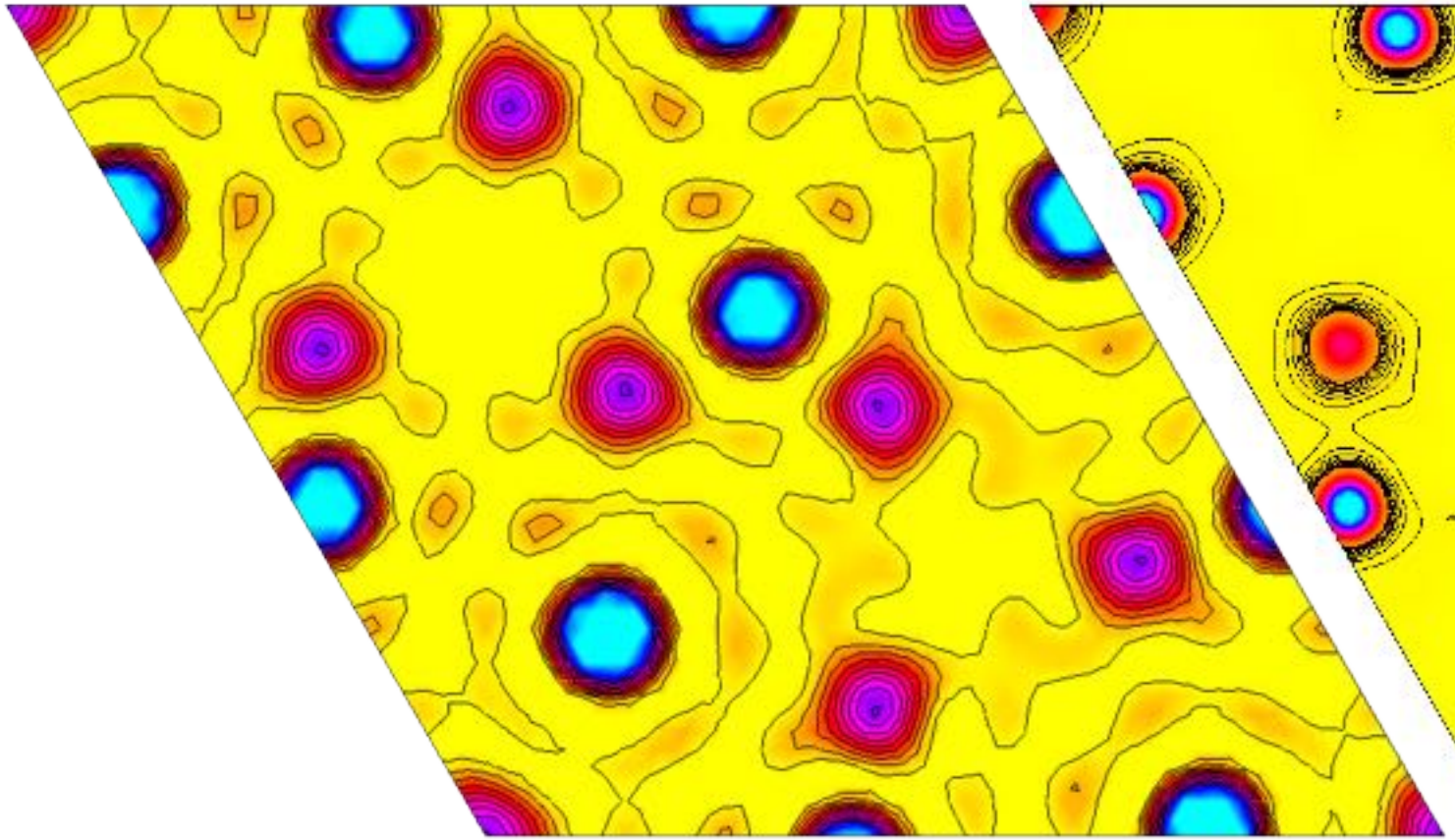

Fourier Synthesis

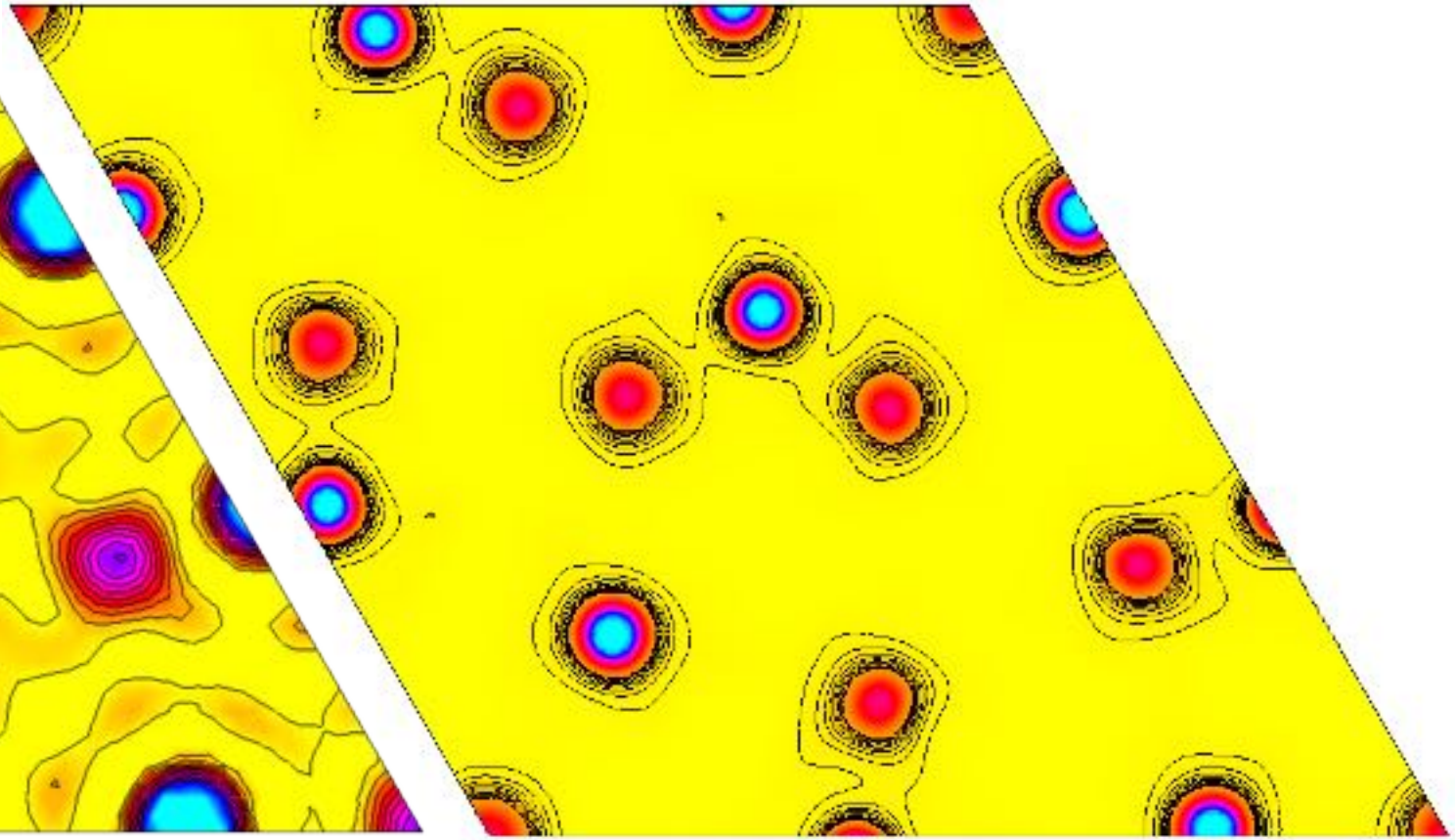

Maximum Entropy Method

# Fourier Synthesis of F-Apatite

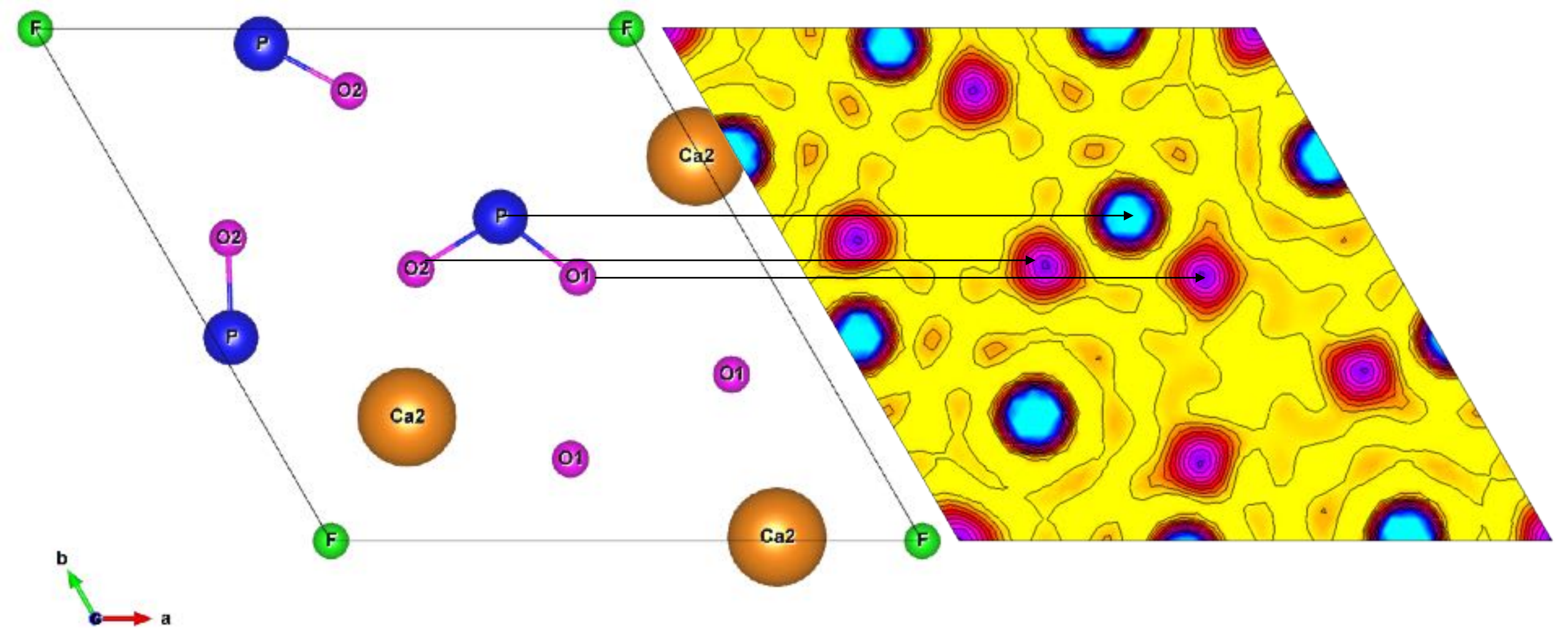

# Maximum Entropy Method of F-Apatite

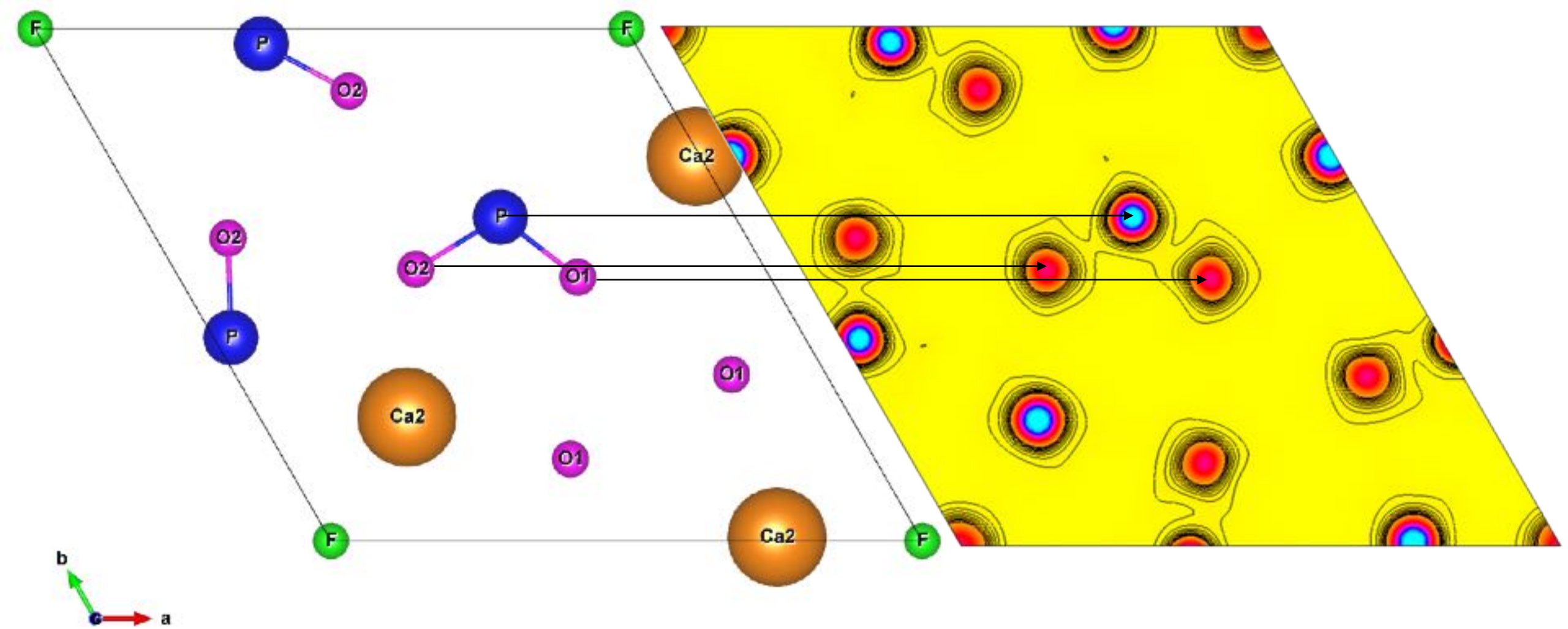

# Visualizing crystal structure evolution of electrode materials upon doping and during charge/discharge cycles in lithium-ion batteries

Dongwei Ma [1,*], Jing Yang [4,5], Maykel Manawan [1,6], Chenglu Yang [1], Jichuil Li [1], Yongzi Liang [4], Tina Feng [3], Yong Wei Zhang [2], Ji Hong Pan [1,7,8,9]

https://doi.org/10.1016/j.xpro.2021.101099
Ma, D., et. al. (2022) STAR Protocols 3, 101099

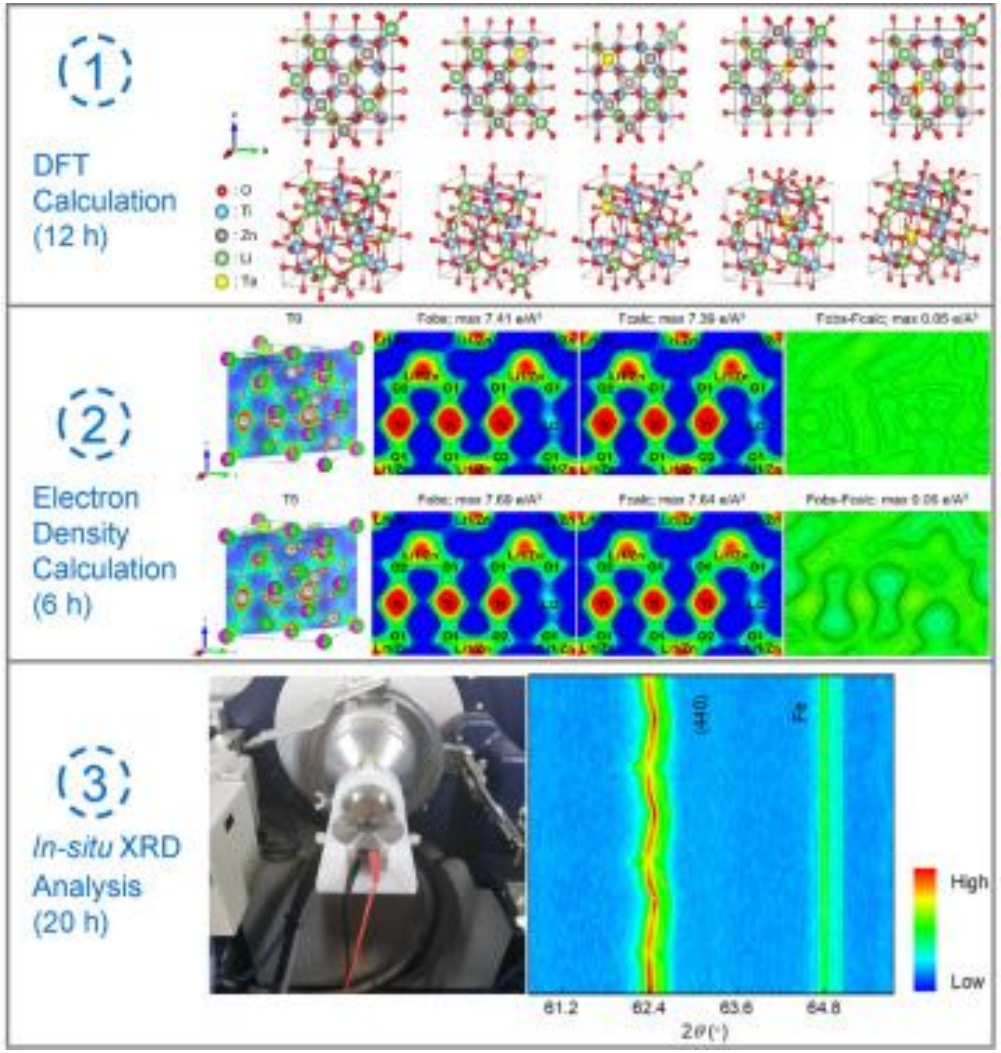


## Highlights

- Monodisperse $Ta^{5+}$-doped $Li_2ZnTi_3O_8$ spheres from $TiO_2$ spheres as self-template
- DFT and electron density calculations for crystal structure parameters
- *In-situ* XRD analysis to visualize crystal structure evolution of electrodes

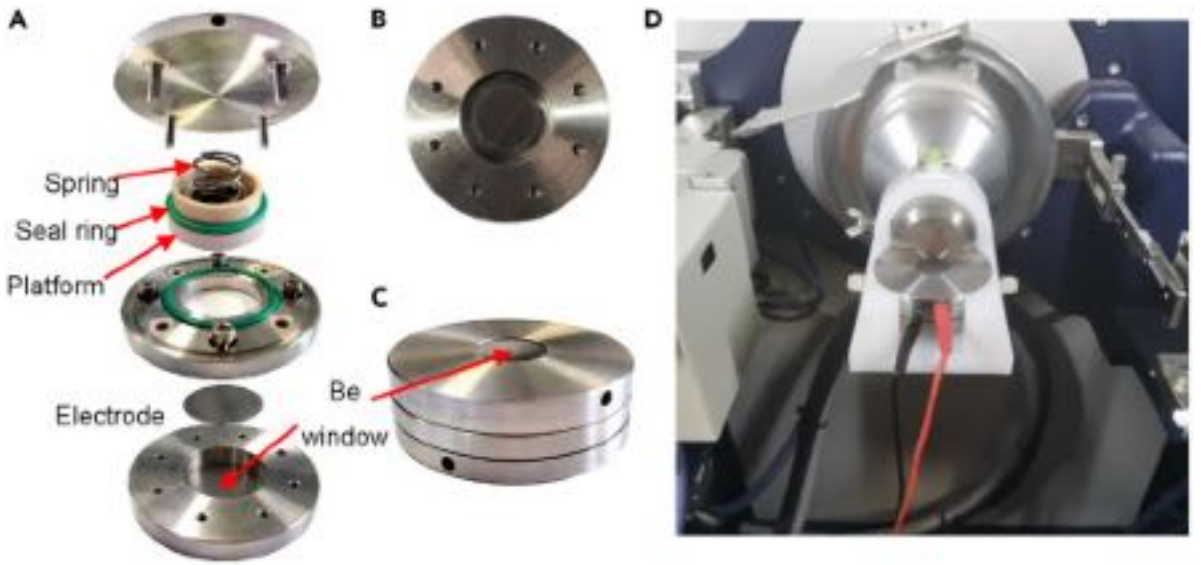

# Finding Li in Li2ZnTi3-xTaxO8 (x = 0, 0.05)

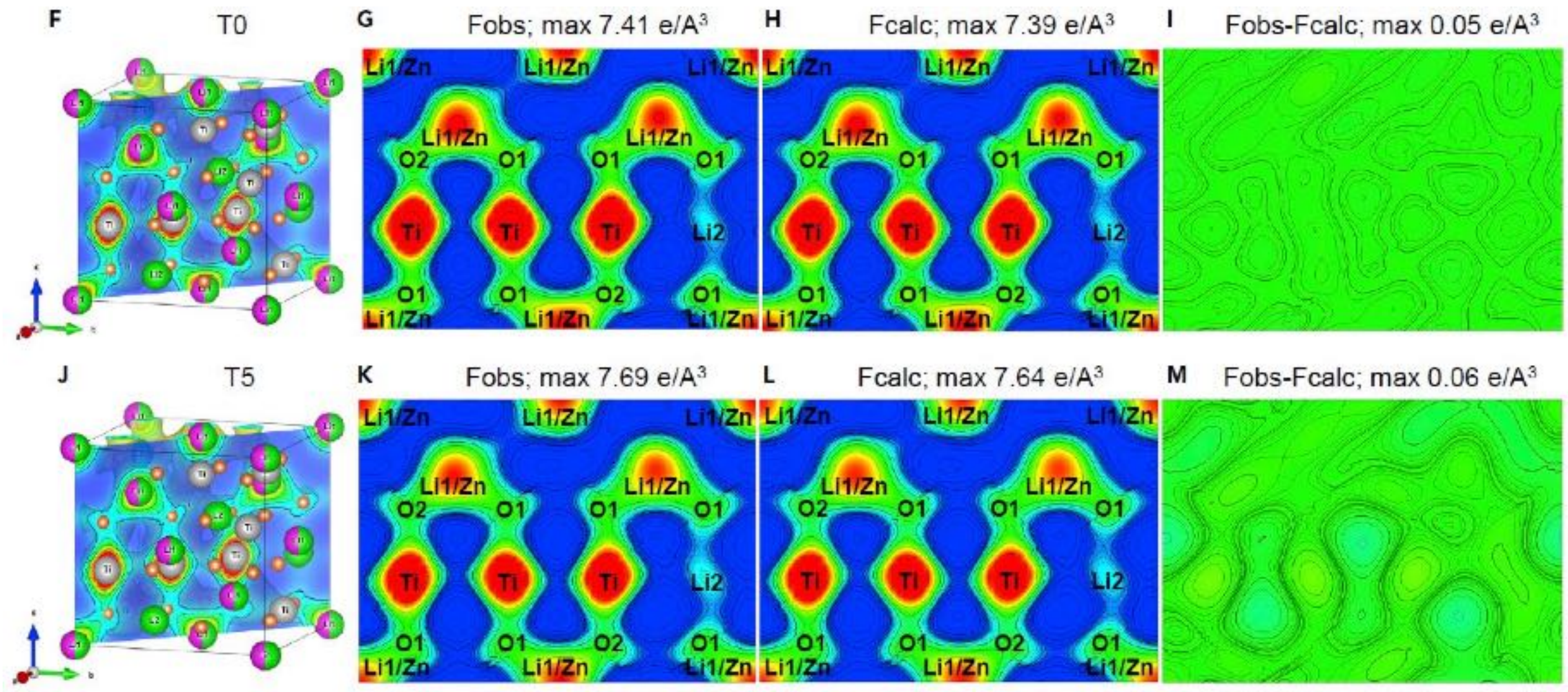


Ma, D., et. al. (2022) STAR Protocols 3, 101099

# Visualizing lithium ions in the crystal structure of $Li_3PO_4$ by *in situ* neutron diffraction

M. Manawan, E. Kartini and M. Avdeev

https://doi.org/10.1107/S1600576721008700

Manawan, M., Kartini, E., Avdeev, M. (2021) J. Appl. Cryst. **54**, 1409–1415

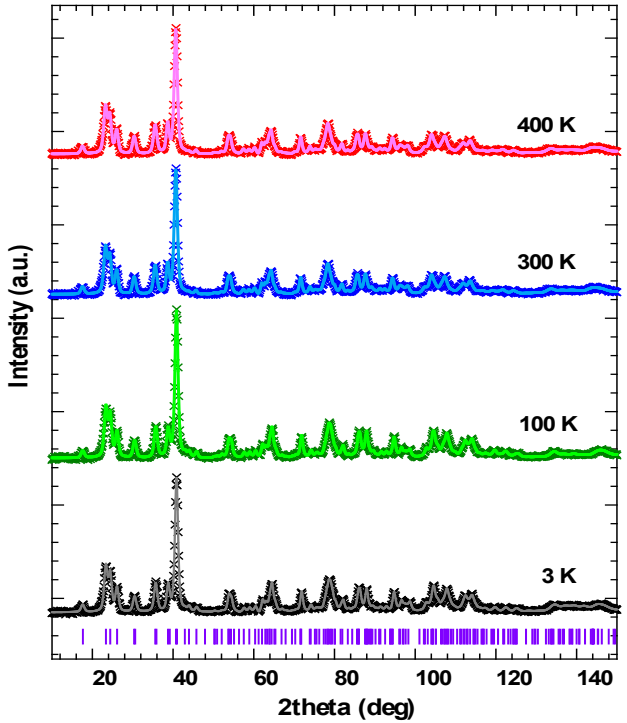


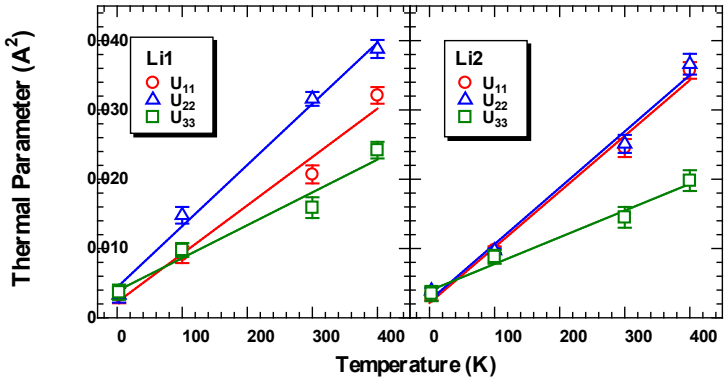


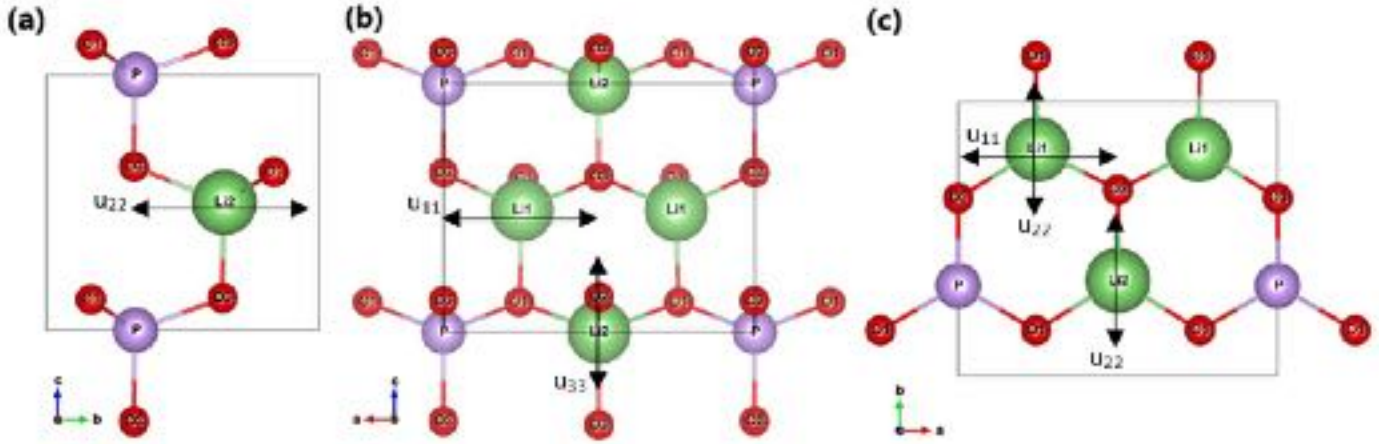


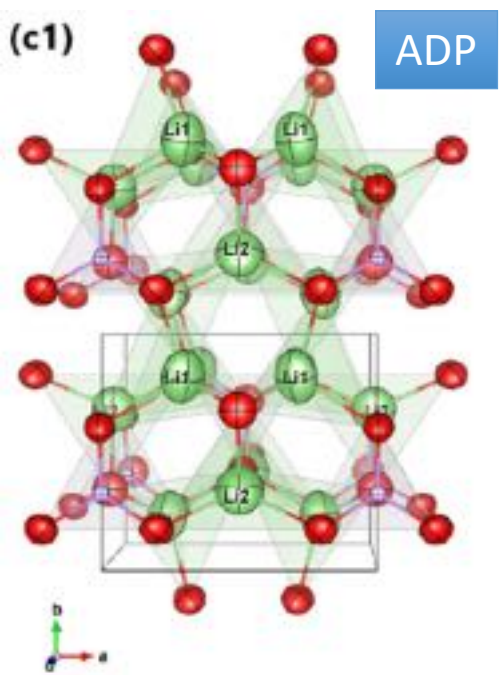


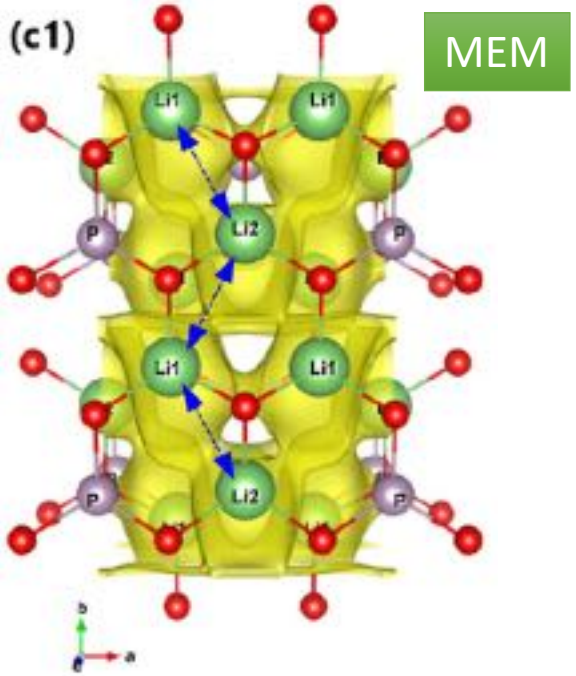


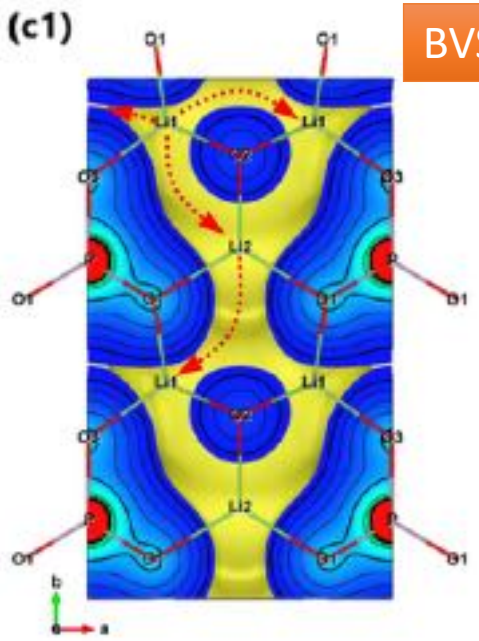

# Li pathway in Li3PO4

3K

100K

300K

400K

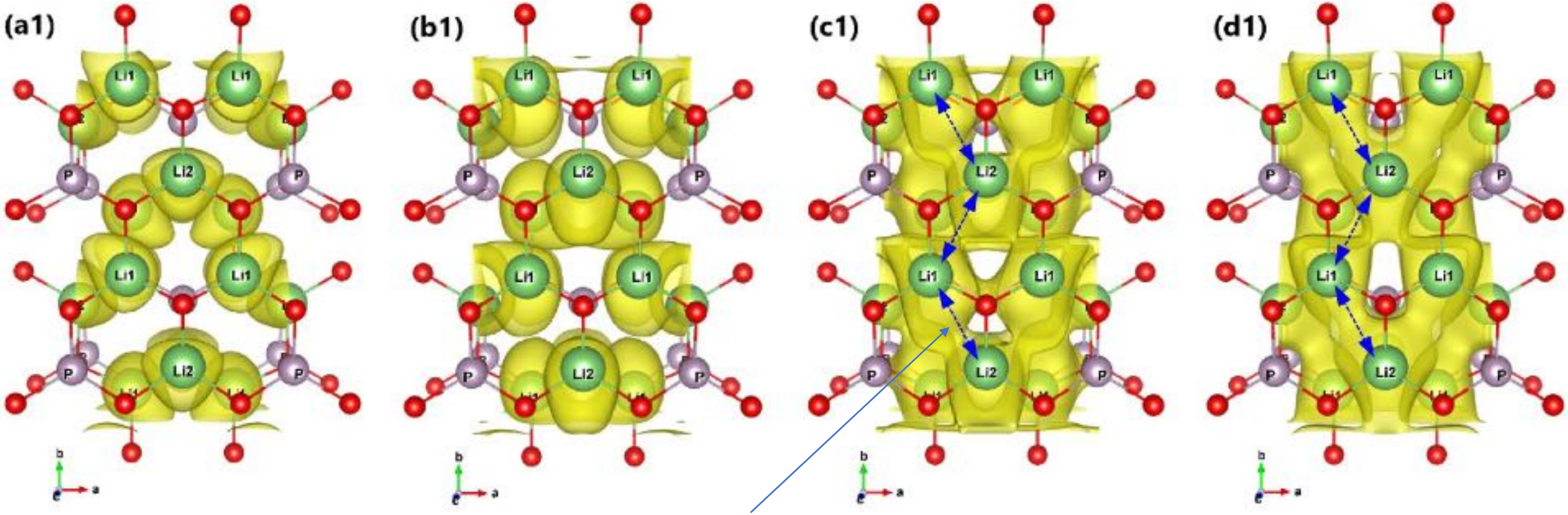


Li diffusion pathway

Manawan, M., Kartini, E., Avdeev, M. (2021) J. Appl. Cryst. **54**, 1409–1415

# Li tunnel in TiNb2O7 (Anode)

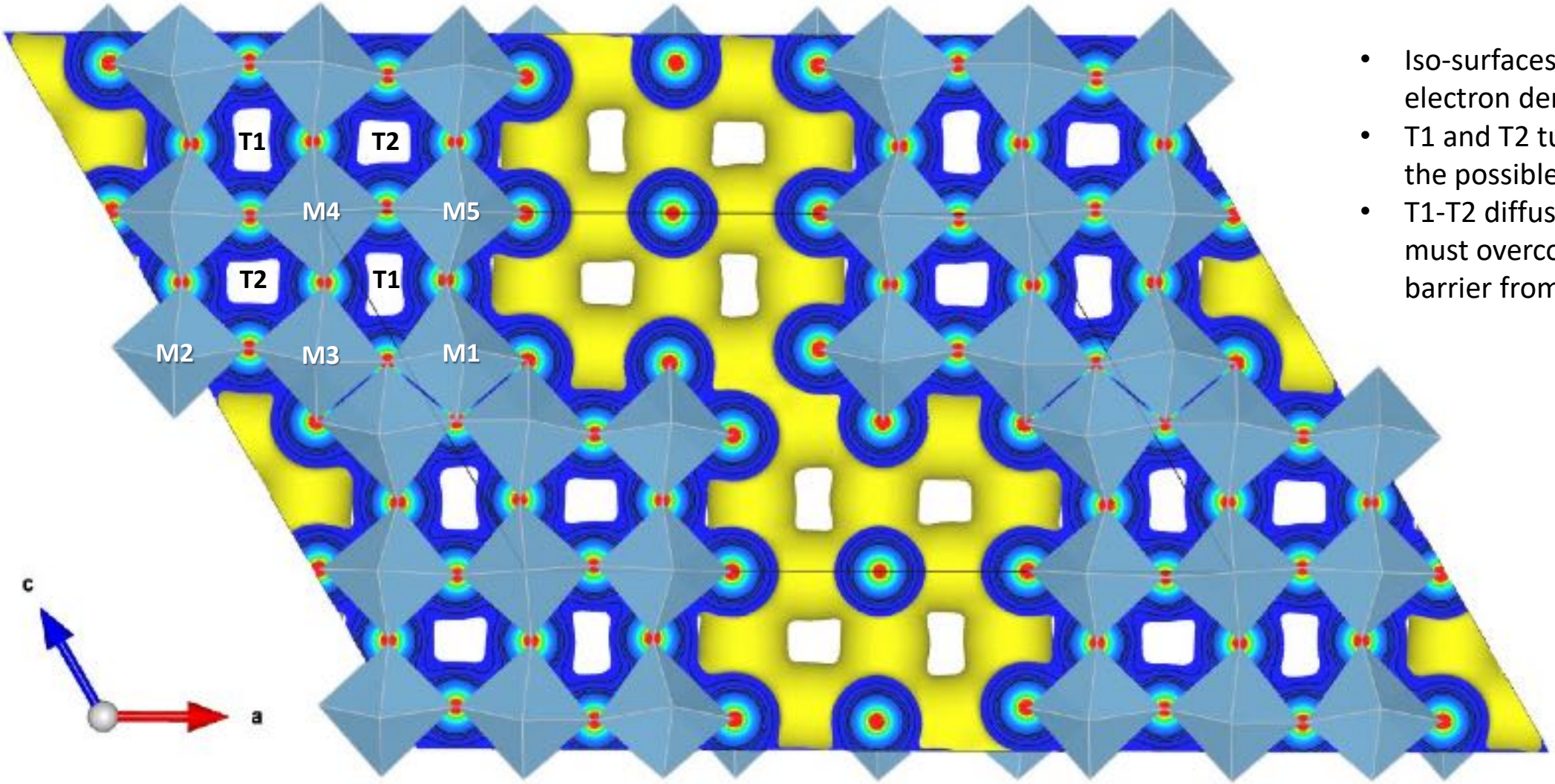


- Iso-surfaces (yellow) is the electron density value of 1 e/Å$^{-3}$
- T1 and T2 tunnels along *b*-axis is the possible Li-ion pathway
- T1-T2 diffusion also possible but must overcome the energy barrier from oxygen atom

Manawan, M., et.al. (2022) recent work

# Oxygen pathway in PLNCG

27 °C

395.4 °C

606.6 °C

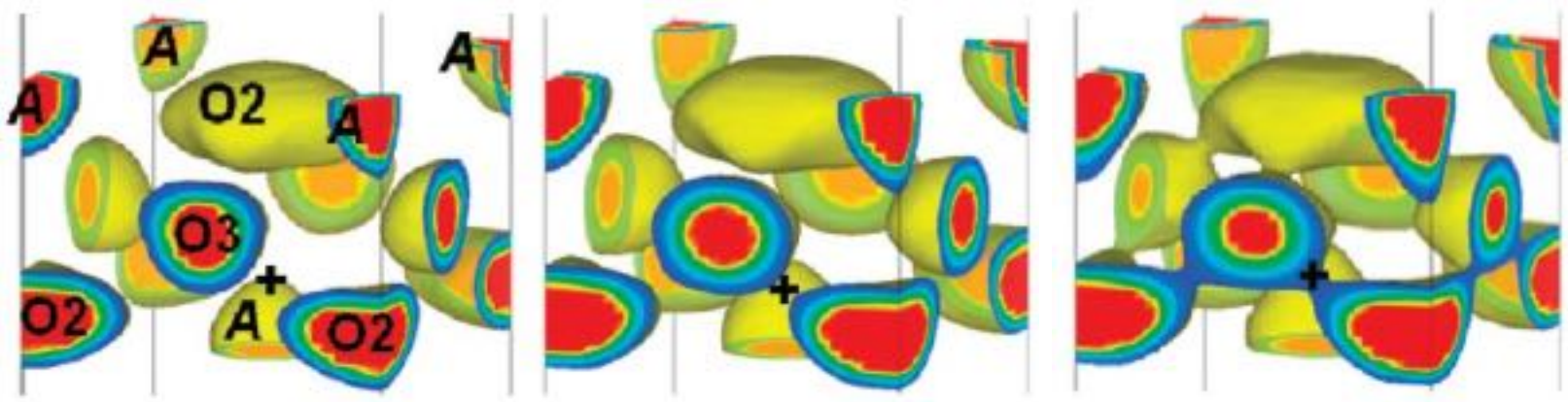


Equinuclear density surface at 0.05 fmÅ$^{-3}$ and nuclear density distribution on the (100) planes of (PLNCG) at different temperatures, which indicates the diffusional pathway of oxide ions in the crystal lattice of PLNCG.

The color scale denotes the values of nuclear density on the (100) planes of PLNCG. A denotes a (Pr,La) atom. The oxide ions diffuse through the oxygen O2-O3-O2 atomic sites. The cross (+) shows the bottleneck for the diffusional pathway between the oxygen O2 and O3 sites. The nuclear density at the bottleneck increases with an increase of temperature

812.8 °C

1015.6 °C

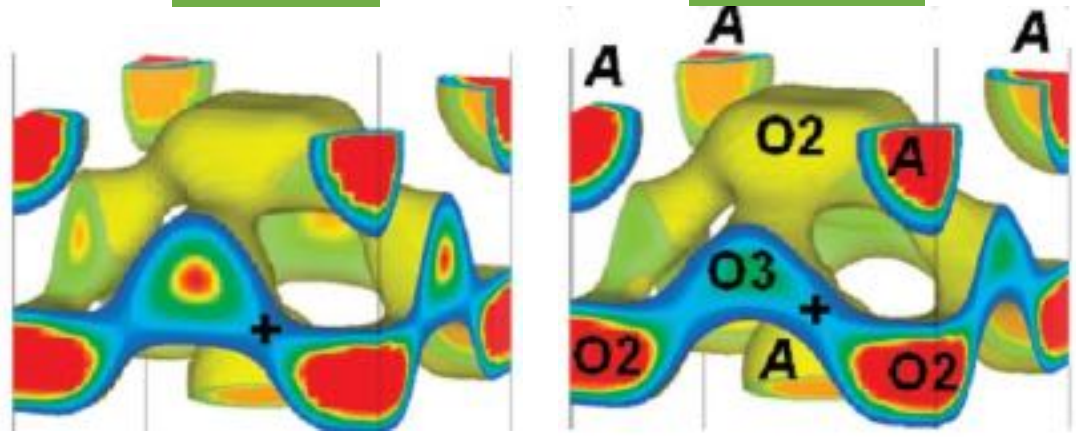


Yashima, M., Sirikanda, N. & Ishihara, T. (2010). J. Am. Chem. Soc. **132**, 2385

# Atomic Disorder in CuI

Split-atom model is the solution for low R factors

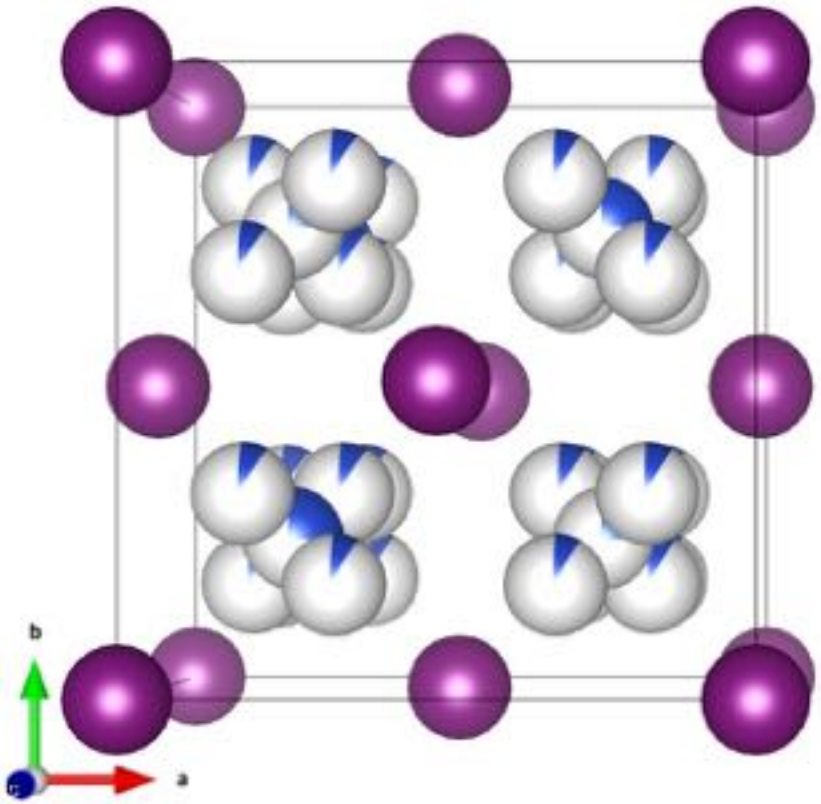


MEM

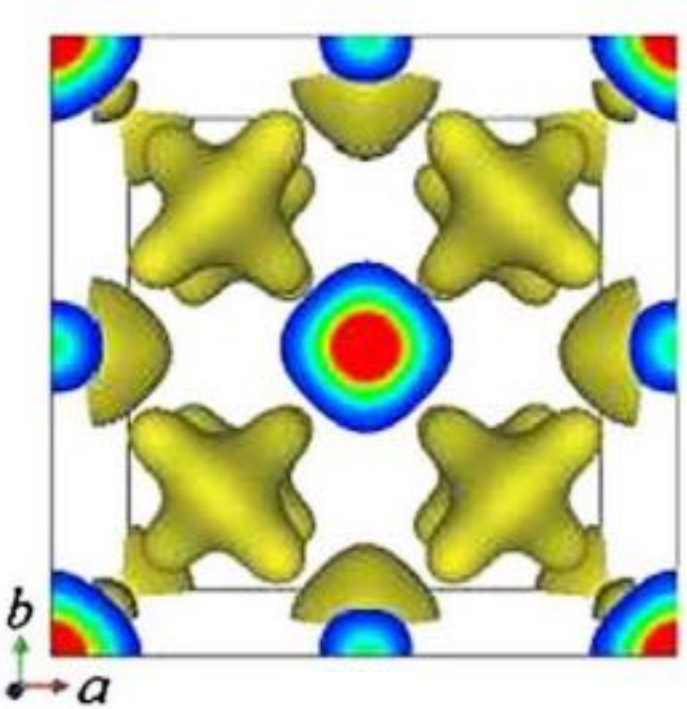


BVS

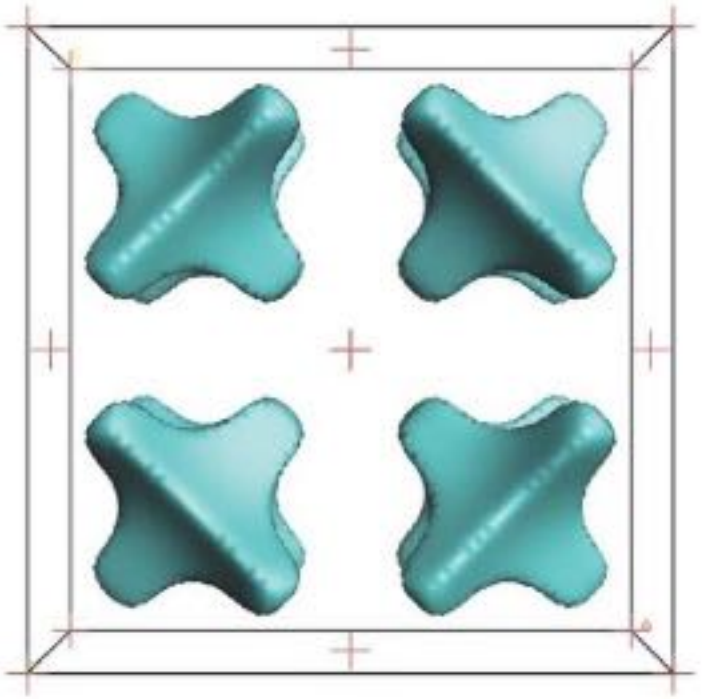

Test Ion $I^{1-}$

Sale, M. & Avdeev, M. (2012) J. Appl. Cryst. **45**, 1054–1056

# Bond Profile in F-Apatite

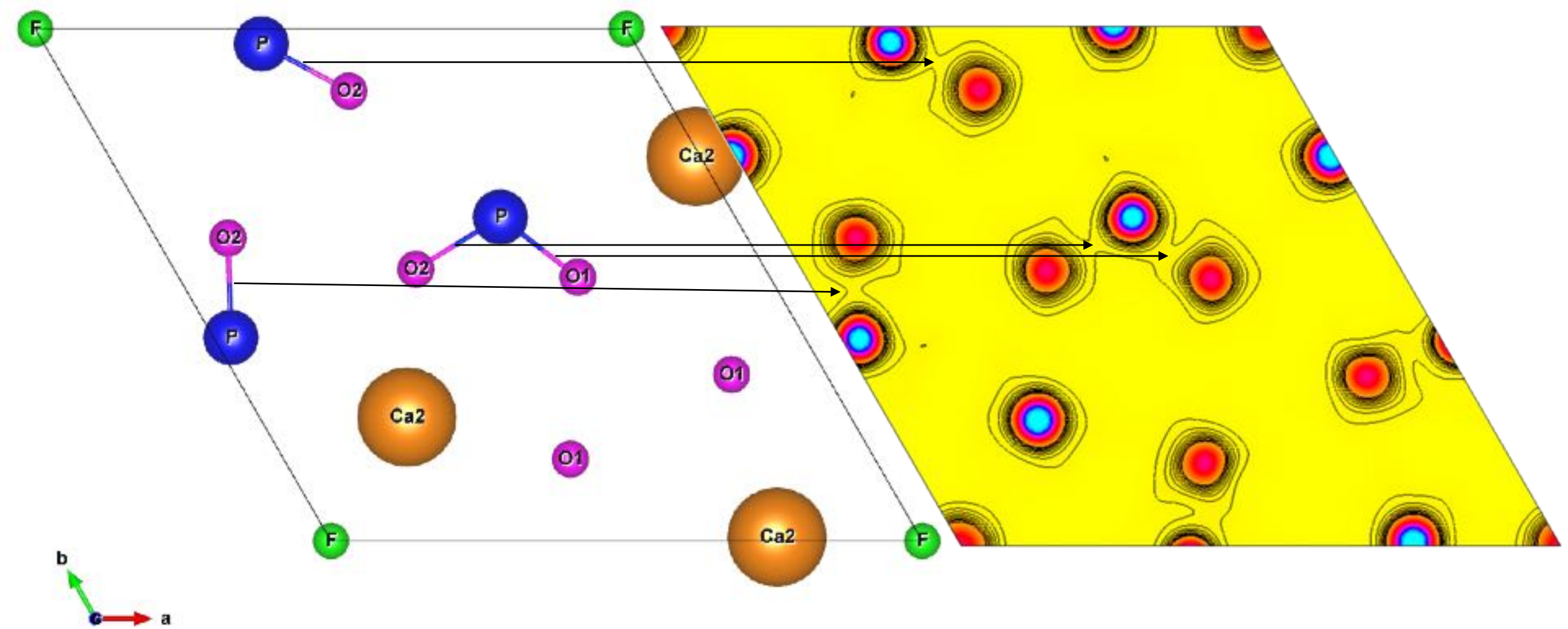

# Electron Density profile of P-O bonds

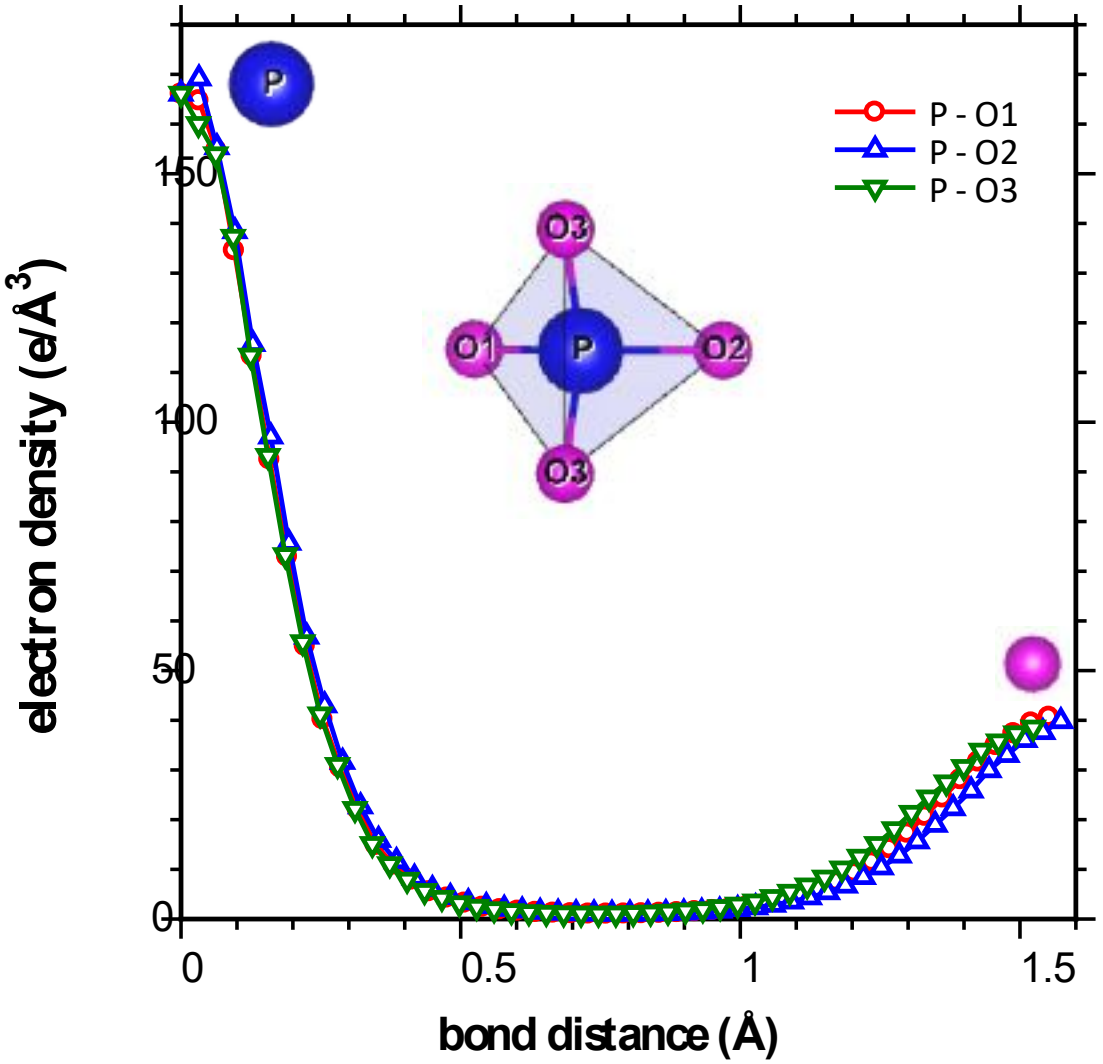


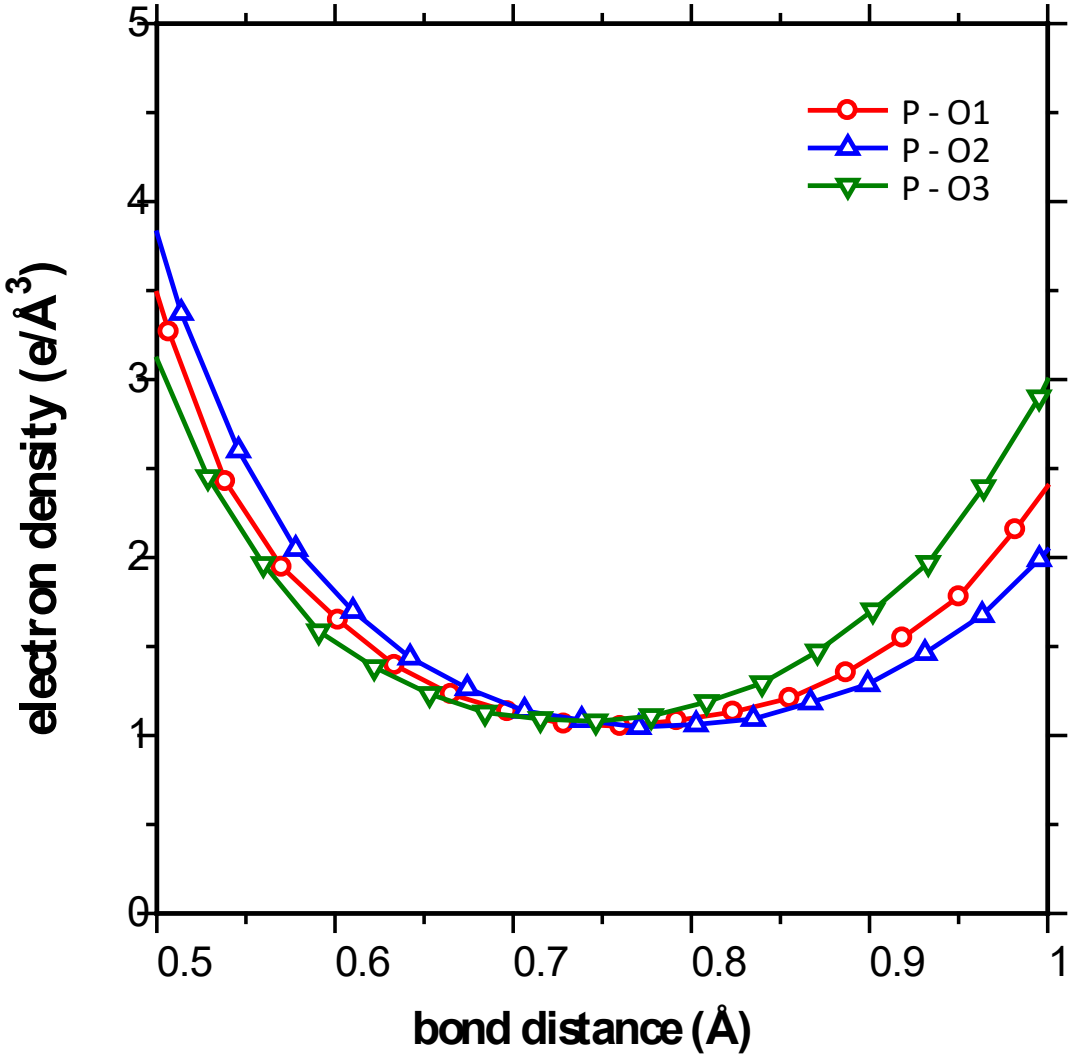

# Electron Density profile of Ca-O bonds

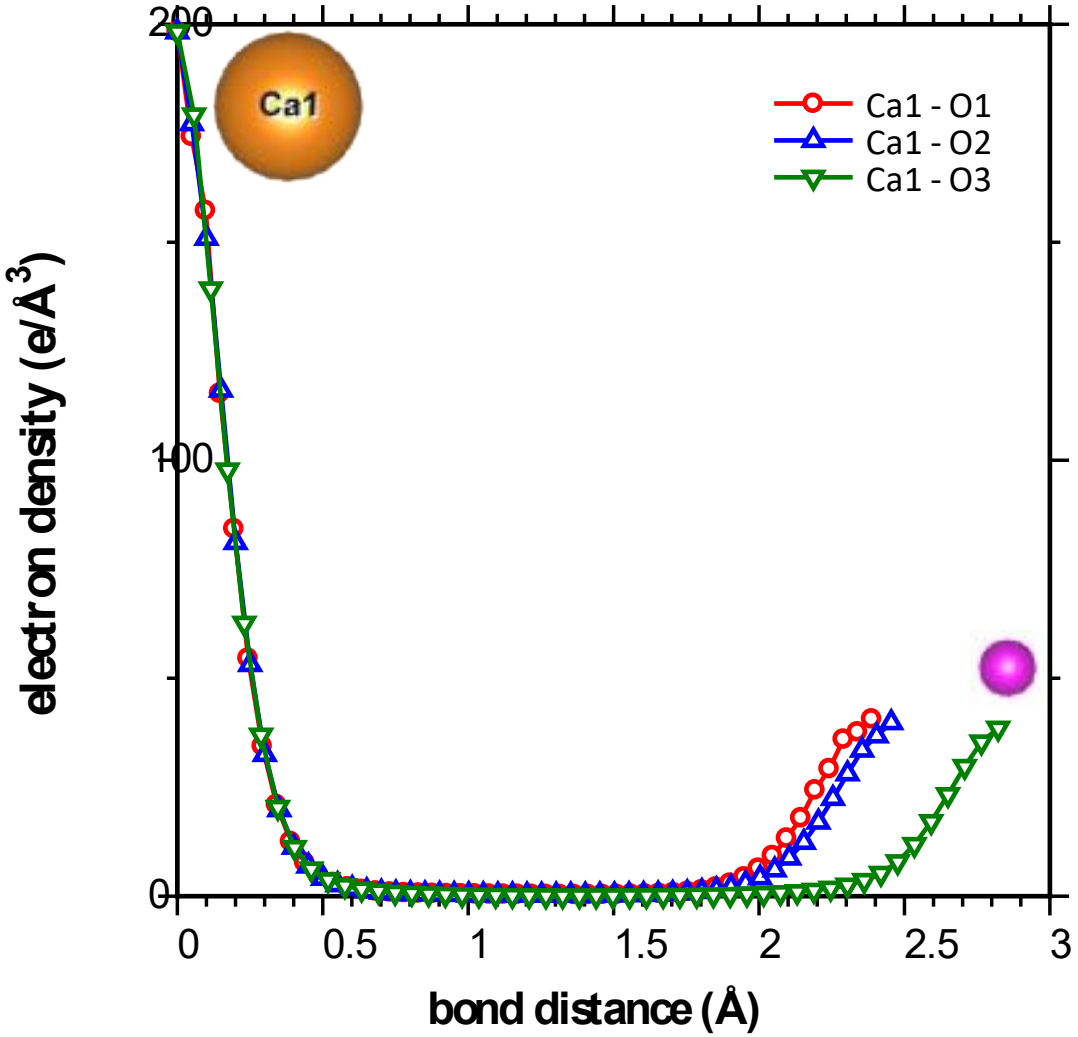


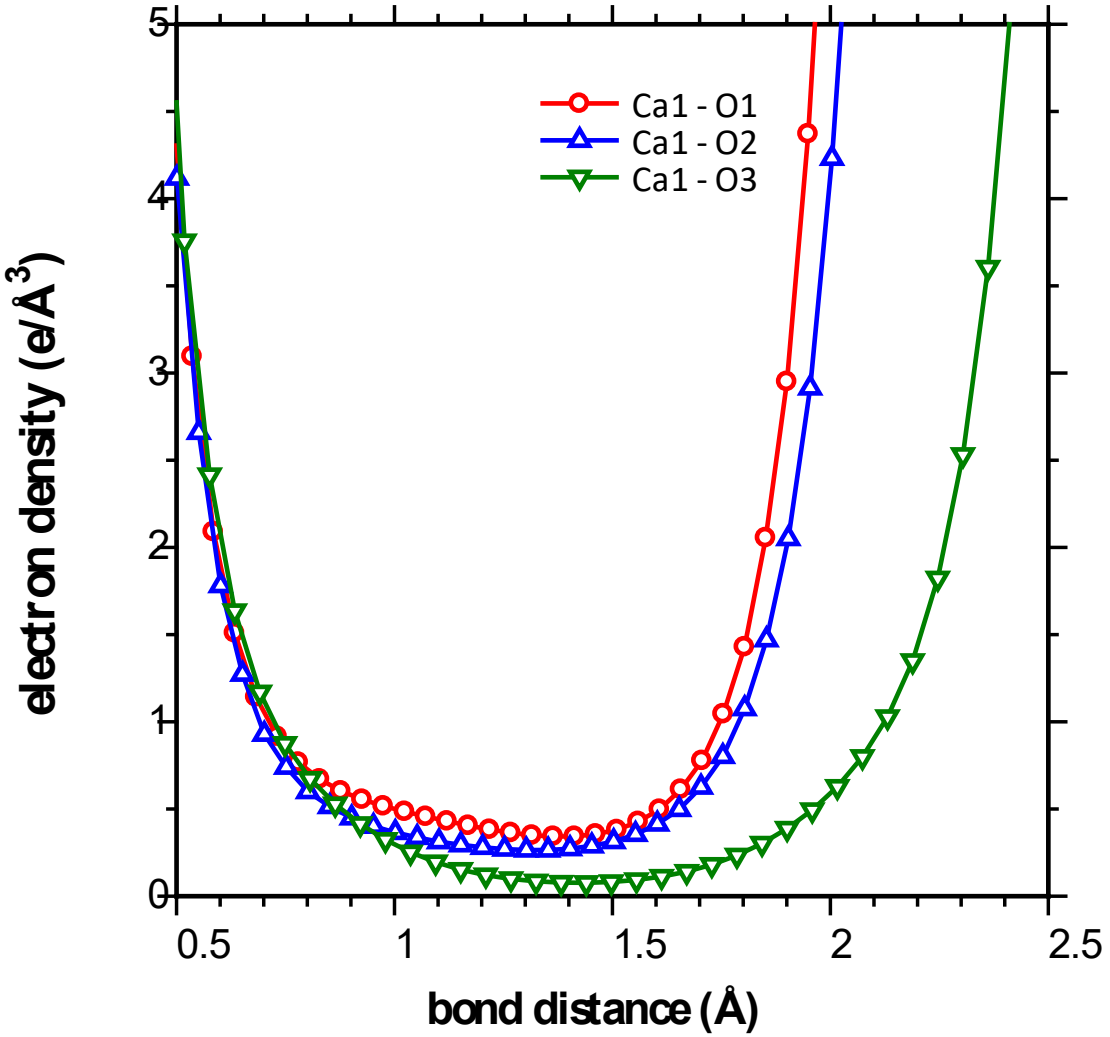

# Electron Density profile of Ca-O/F bonds

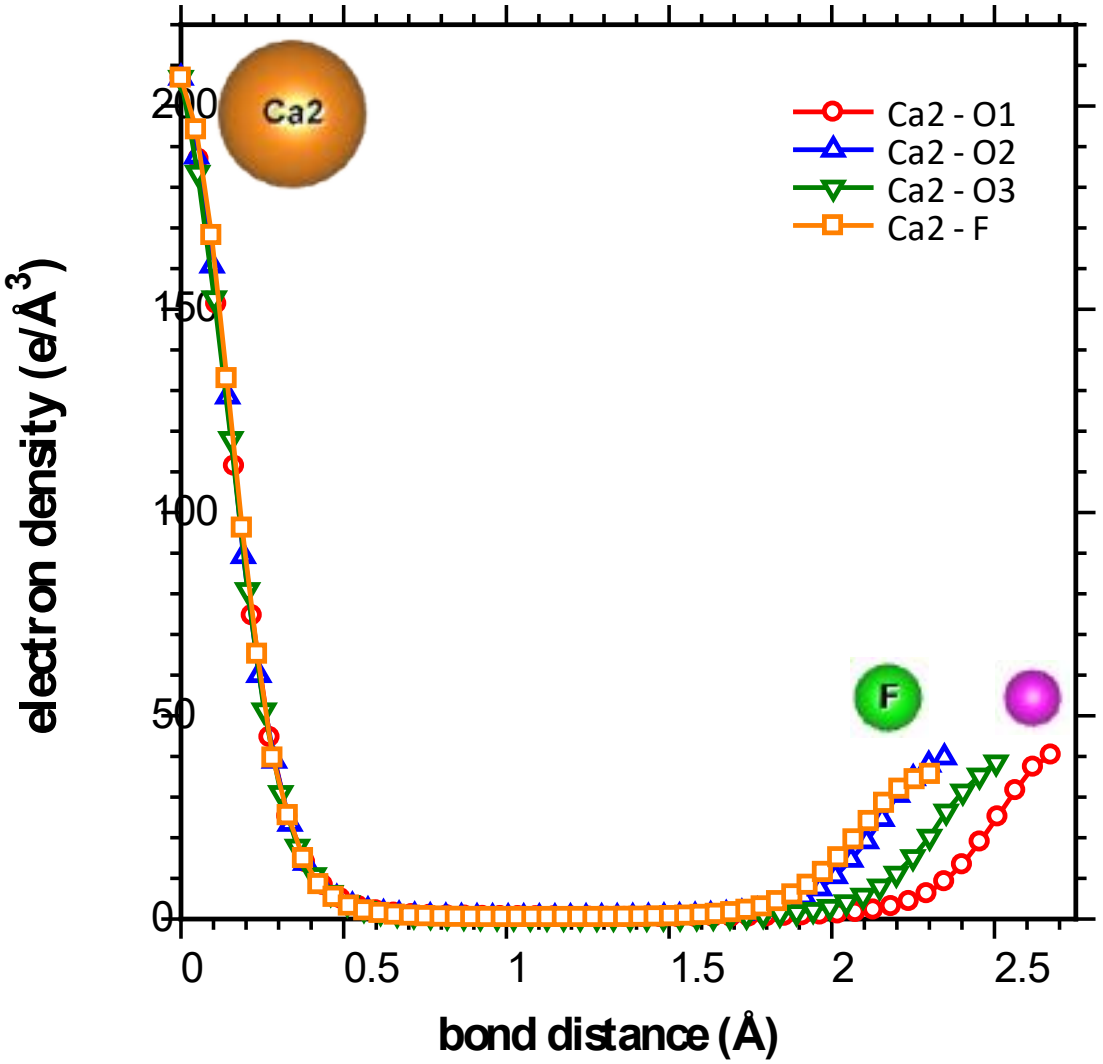


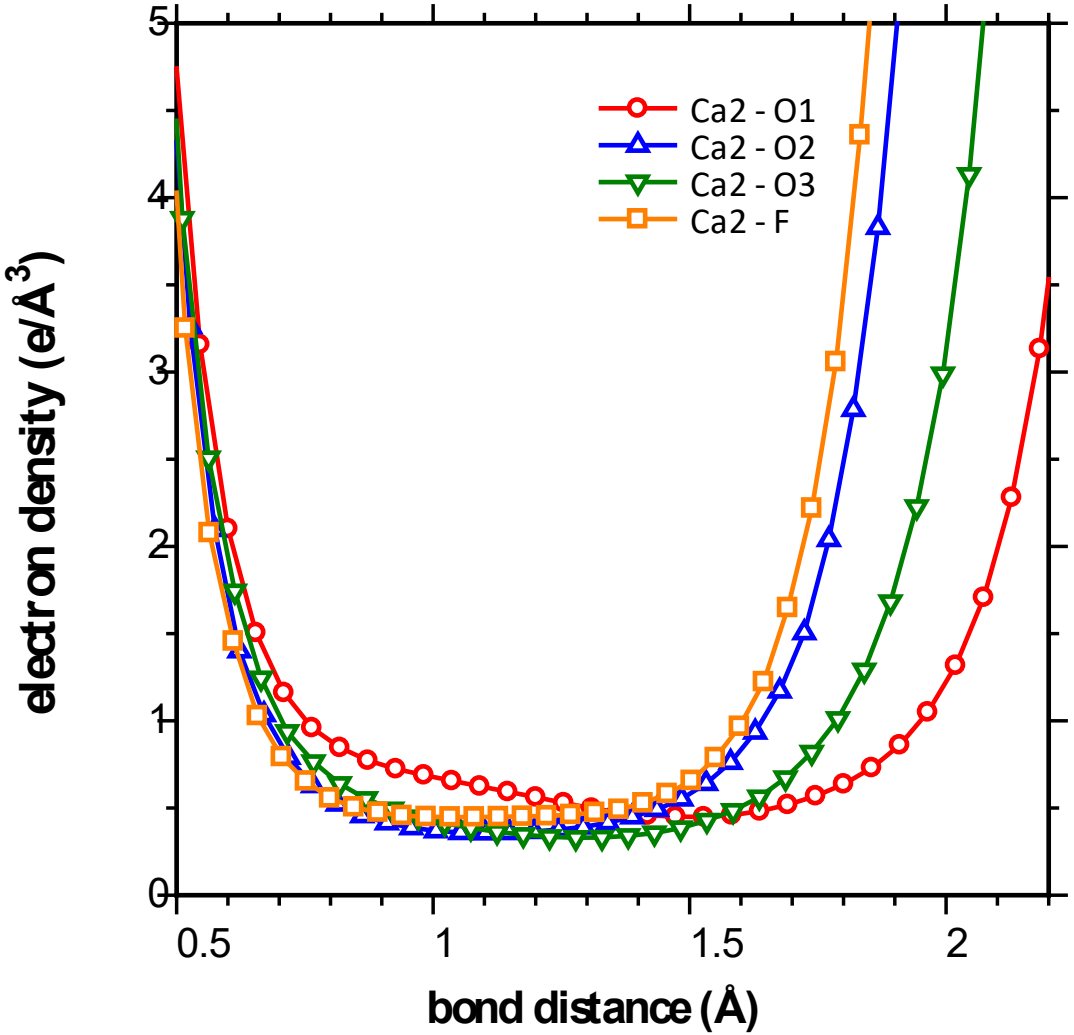

# Some calculation obstacle

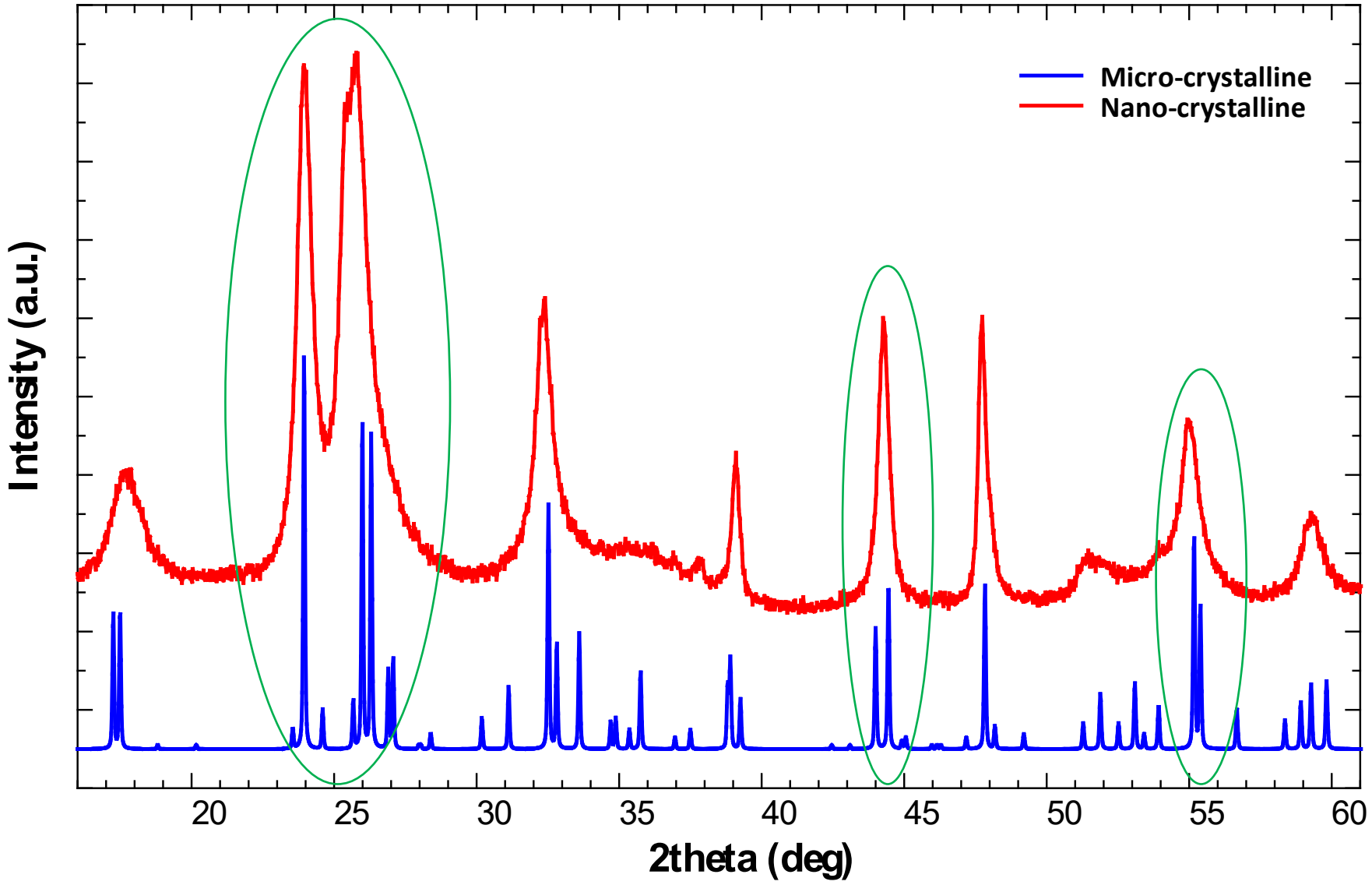


**Problem:**

Highly overlapped peaks in the nano-crystalline sample caused by individual peak broadening. Further, most adjacent peaks are merged.

Solution:

Heat treat the sample to increase the crystallite size and inspect the overlapped peak by comparing with database

# Bond Valence Sum

## Atomic Radii and Interatomic Distances in Metals[1]

By Linus Pauling

normal covalent radii. The available evidence indicates that the differences between single-bond, double-bond, and triple-bond radii are very nearly the same for all atoms,[9] and hence that an expression can be found for a term to be added to the single-bond covalent radius for any atom to give approximately the radius corresponding to another bond type. The carbon–carbon bond distances are 1.542, 1.330, and 1.204 Å. for a single bond, double bond, and triple bond, respectively, the double-bond and triple-bond radius corrections hence being −0.106 and −0.169 Å. The ratio of these numbers is just equal to log 2/log 3; accordingly the bond-type correction may be taken proportional to the logarithm of the bond number, $n$

$$-\Delta R(n) = 0.353 \log n \qquad (1)$$

Here $\Delta R$ is $R(n) - R(1)$, in Å., and $n$ is the number of shared electron pairs involved in the bond. This logarithmic relation is, of course, to be expected in consequence of the exponential character of interatomic forces.

JACS 69 (1947) 542

Butane

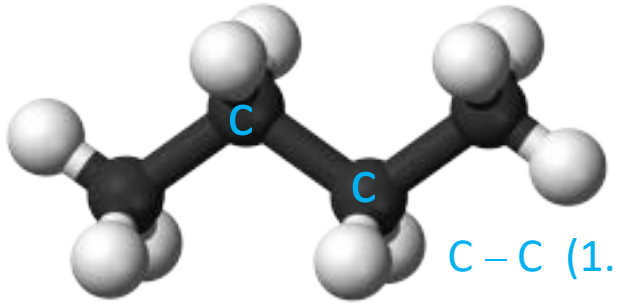


C – C (1.542 Å)

Butene

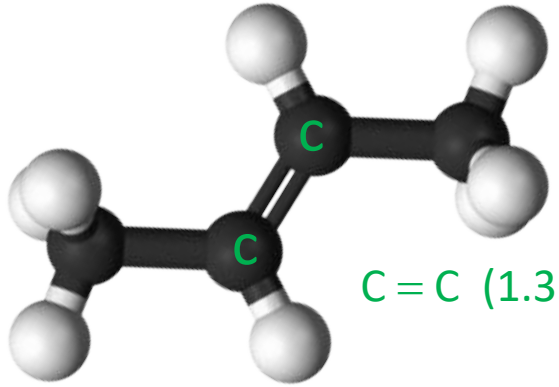


C = C (1.330 Å)

Butyne

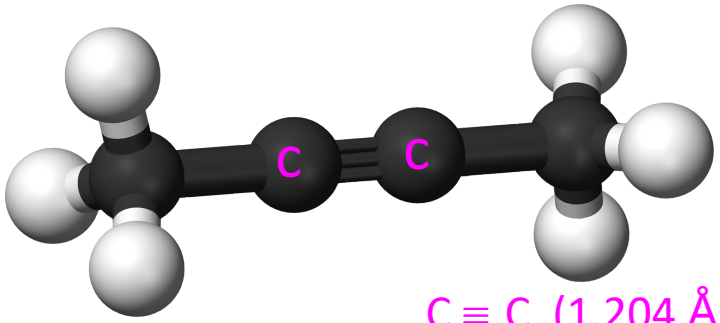


C ≡ C (1.204 Å)

# Bond Valence Sum Landscape

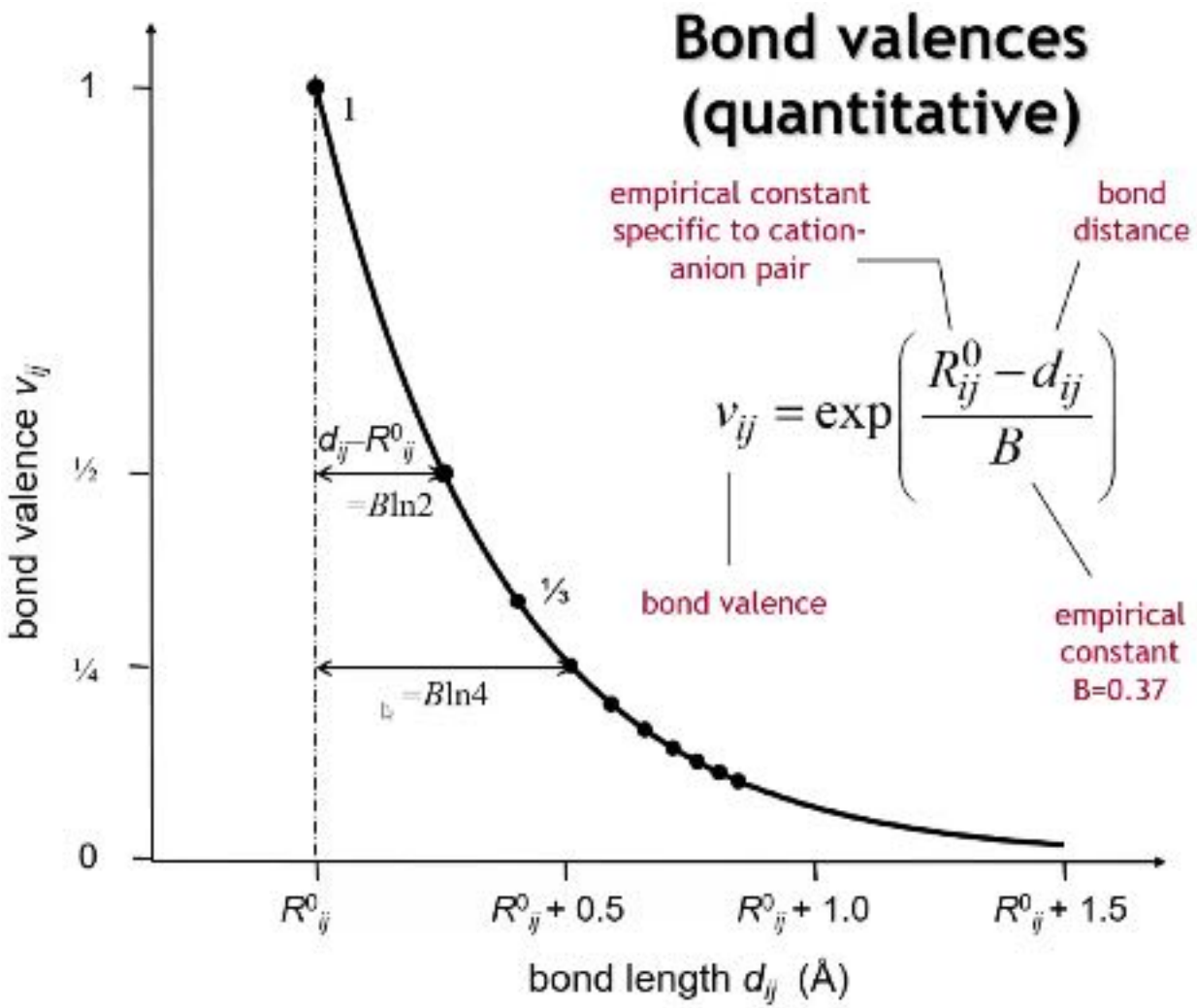


$$\mathrm{BVS} = \sum_{j=1}^{N}\left[m_j \exp\left(\frac{R_0 - d_j}{b}\right)\right], \qquad (1)$$

where $d_j$ is the distance to the $j$th counter-ion site with occupancy $m_j$, $R_0$ and $b$ are tabulated constants which are dependent on the type of test ion and the $j$th neighbour, respectively, and N is the number of counter-ions within the preset cut-off distance.

$$\mathrm{BVEL}_{+/-} = \sum_{j=1}^{N}\left(m_j D_0\left\{\exp\left[\alpha\left(R_{\min} - d_j\right)\right] - 1\right\}^2 - 1\right), \qquad (2)$$

$$\mathrm{BVEL}_{+/+,-/-} = \sum_{j=1}^{N}\left\{\mathrm{ConvEV}\frac{m_j}{d_j}\frac{|V_{TI}||V_j|}{\left(n_{qnTI}n_{qnj}\right)^{1/2}} \times \left[\mathrm{erfc}\left(\frac{d_j}{\rho}\right) - \mathrm{erfc}\left(\frac{d_{\mathrm{cutoff}}}{\rho}\right)\right]\right\}, \qquad (3)$$

$$\rho = \rho_f\left(r_{TI} + r_j\right), \qquad (4)$$

where dj, mj and N have the same meaning as in equation (1), $D_0$, $R_{min}$ and are all constants that are dependent on both the type of test ion and the type of jth neighbour, ConvEv is the conversion factor from inverse length to energy in eV, $V_{TI}$ / $J_j$ and $n_{qnTI}$/ $n_{qnj}$ are the oxidation states and quantum numbers of the test ion and its $j$th neighbour, respectively, erfc is the complementary error function, $d_{cutoff}$ is the distance after which the erfc tail is removed, f is a constant equal to 0.74, and $r_{TI}$ and $r_j$ are tabulated covalent radii.

Sale, M. & Avdeev, M. (2012) J. Appl. Cryst. **45**, 1054–1056

# Li pathway in Cathode Materials

- Layered Structure
- $LiCoO_2$ (LCO)
- 2D Li transport pathways

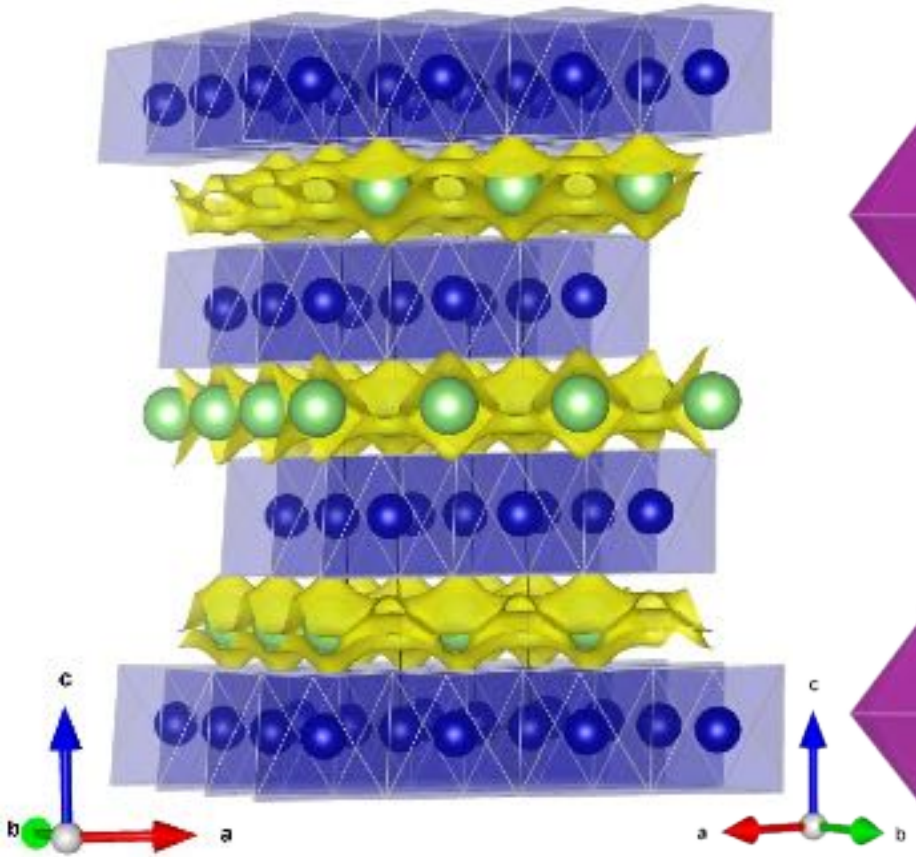


- Spinel Structure
- $LiMn_2O_4$ (LMO)
- 3D Li transport pathways

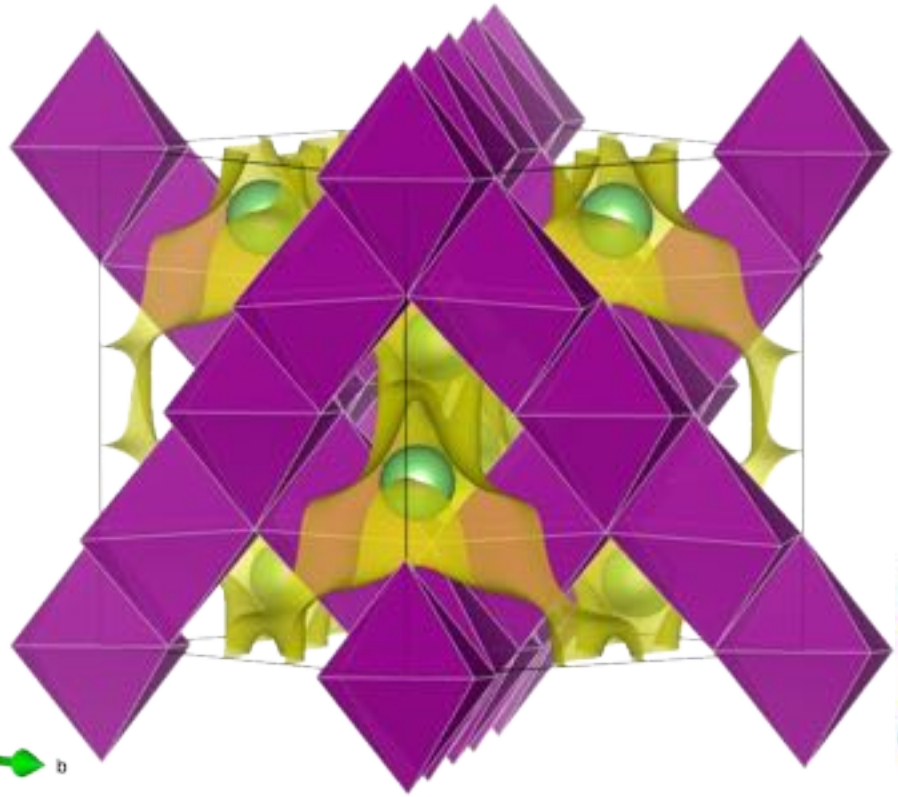

- Olivine Structure
- $LiFePO_4$ (LFP)
- 1D Li transport

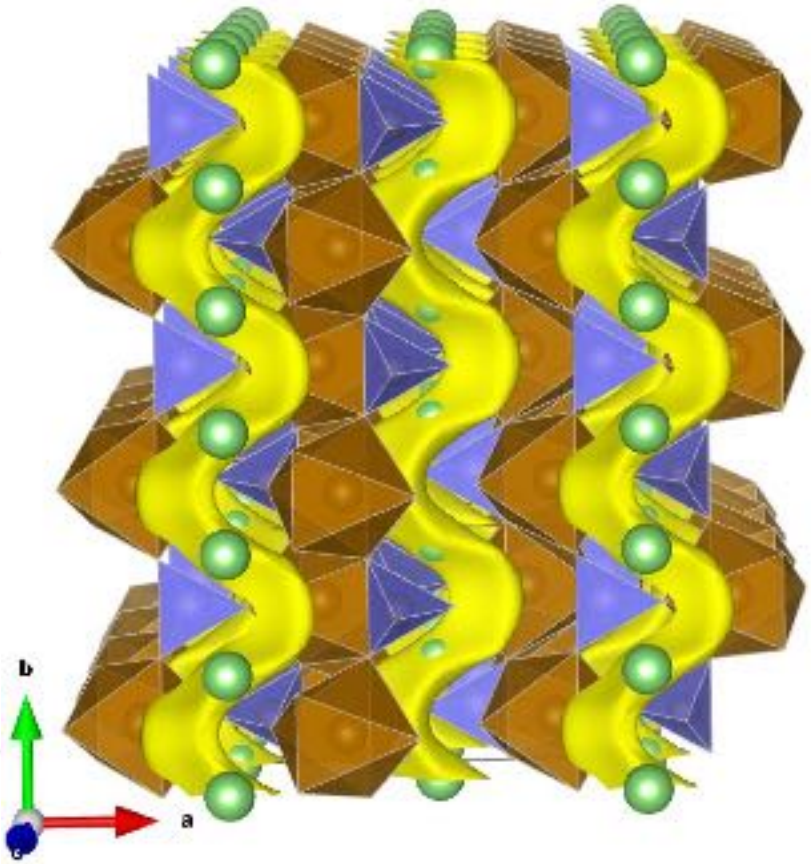

# Li tunnel in TiNb2O7 (Anode)

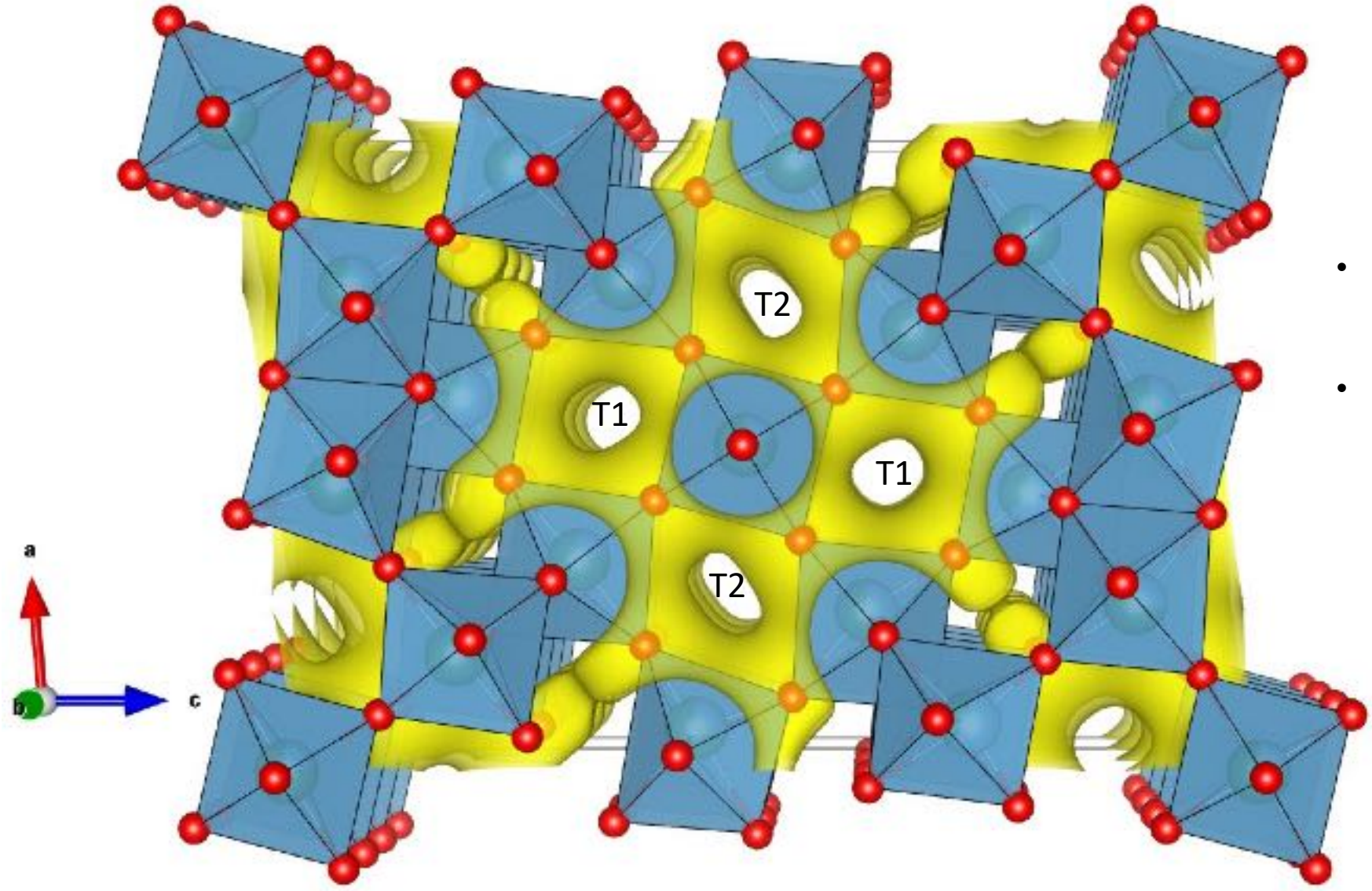


- Iso-surfaces (yellow) is valence (BV) mismatch that identify as low BV barrier (0.2 v.u.)
- T1 and T2 tunnels along *b*-axis is the possible Li-ion pathway

Manawan, M., et.al. (2022) unpublished work

# Li pathway in Li3PO4

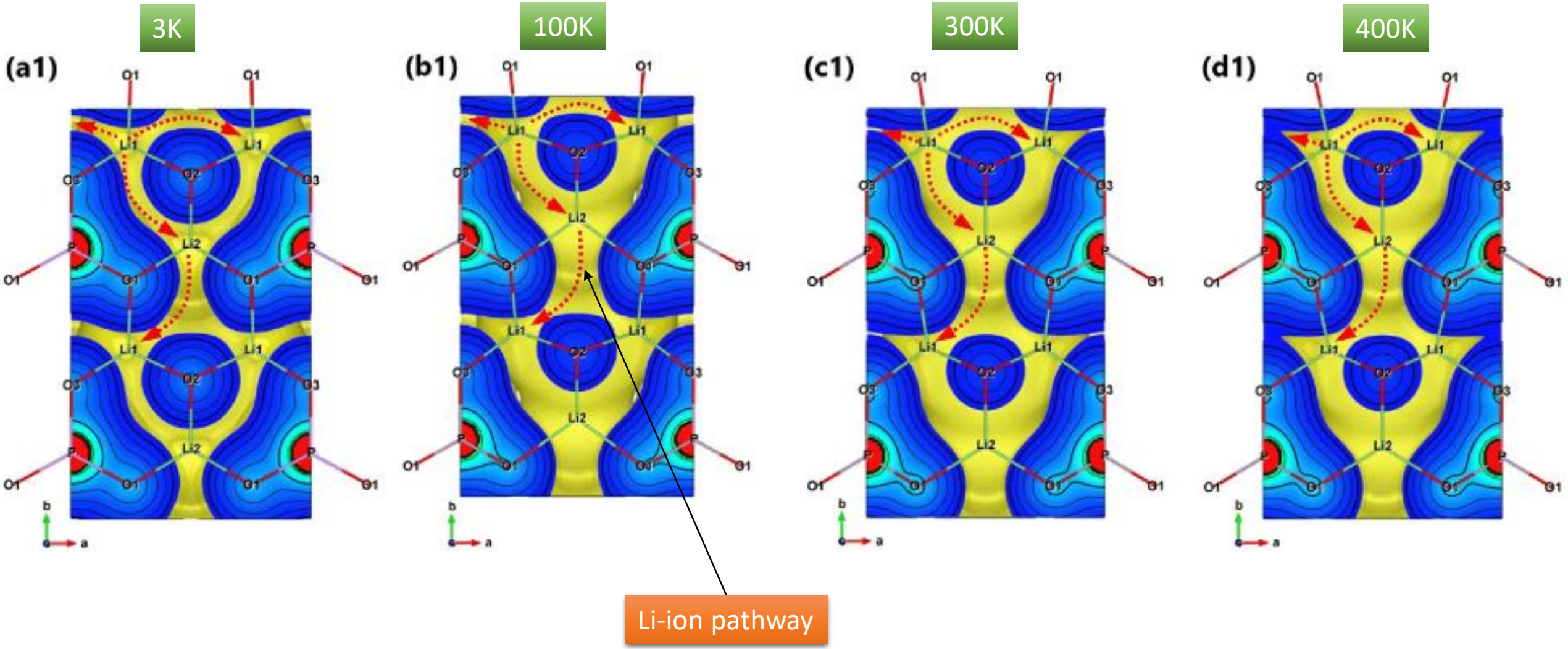


Manawan, M., Kartini, E., Avdeev, M. (2021) J. Appl. Cryst. **54**, 1409–1415

# Site Potential & Madelung Energy

**Table 1** Charge Distributions and Site Potentials ($Å^{-1}$) in $TiNb_2O_7$

| Atom | % Titanium * | Average site charge | Site potential (observed distribution) | Site potential (random distribution) |
|---|---|---|---|---|
| M1 | 33.8 (1.1) | +4.66 | −3.25 | −3.20 |
| M2 | 64.5 (1.3) | +4.35 | −3.16 | −3.19 |
| M3 | 26.0 (1.3) | +4.74 | −3.44 | −3.35 |
| M4 | 14.0 (1.9) | +4.86 | −3.99 | −4.04 |
| M5 | 20.6 (1.4) | +4.79 | −3.56 | −3.59 |

* Estimated standard deviations in parentheses.

Coulombic lattice energy for observed distribution = 51,364 kJ $mol^{-1}$; random distribution = 51,230 kJ $mol^{-1}$.

Both compounds show a striking degree of cation ordering (Tables 1 and 2). In $TiNb_2O_7$ the titanium occupancy in the centre of the block (M4) is 14%, while that in the corner site M2 is 64.5%. A similar distribution of titanium obtains in ortho-$Ti_2Nb_{10}O_{29}$ with 4.5% in M4 and 40.0% in M2. The general features of the average charge distribution in these structures can be understood by considering the way in which local charge balance might be maintained. Thus, the central atom M4 is coordinated by six oxygen atoms each of which is shared with only one other cation as in the $ReO_3$ structure; this site requires a highly charged cation.

Cheetham, A. K. & Von Dreele, R. B. (1973). Nature, Phys. Sci. **244** (139), 139

```
*********************************
*   MADEL written by K. Kato    *
*   and modified by F. Izumi    *
*   v1.31, July 23, 2013        *
*********************************

Ti Nb2 O7
Radius of an ionic sphere:  1.30 Å
Reciprocal-space range:  4.00 Å**(-1)
Number of symmetry operations:   4
Number of atoms in the asymmetric unit:  16
Inversion center at the origin:   1

Lattice parameters:   20.3510   3.8010  11.8820   90.000  120.190
90.000

Potentials of sites in the asymmetric unit

          Charge       W         x         y         z          phi
Ti1      4.660000 0.500000 0.078600 0.000000 0.636800 -3.170284E+00
Ti2      4.350000 0.500000 0.293100 0.000000 0.367600 -3.129874E+00
Ti3      4.740000 0.500000 0.888900 0.000000 0.630700 -3.428315E+00
Ti4      4.860000 0.250000 0.000000 0.000000 0.000000 -3.943042E+00
Ti5      4.790000 0.500000 0.185600 0.000000 0.006000 -3.605408E+00
O1      -2.000000 0.500000 0.173800 0.000000 0.585900  2.146823E+00
O2      -2.000000 0.500000 0.373000 0.000000 0.580000  1.953267E+00
O3      -2.000000 0.500000 0.596700 0.000000 0.621000  2.107665E+00
O4      -2.000000 0.500000 0.790900 0.000000 0.618800  1.817720E+00
O5      -2.000000 0.500000 0.250800 0.000000 0.197300  1.821839E+00
O6      -2.000000 0.500000 0.709400 0.000000 0.002200  1.859515E+00
O7      -2.000000 0.500000 0.899600 0.000000 0.986300  1.595536E+00
O8      -2.000000 0.500000 0.025000 0.000000 0.418800  2.053741E+00
O9      -2.000000 0.500000 0.875300 0.000000 0.188500  1.791826E+00
O10     -2.000000 0.250000 0.500000 0.000000 0.000000  1.434392E+00
O11     -2.000000 0.500000 0.049500 0.000000 0.197900  1.623398E+00

Electrostatic energy per asymmetric unit
    -27.616809 e**2/Å = -397.67243 eV = -38.369547 MJ/mol
```

5Cu-TiNb2O7 (Dreele)_refined

Oxygen Occ. = 1

```
*******************************
*   MADEL written by K. Kato  *
*   and modified by F. Izumi  *
*   v1.31, July 23, 2013      *
*******************************

 Ti Nb2 O7
 Radius of an ionic sphere:  1.30 Å
 Reciprocal-space range:  4.00 Å**(-1)
 Number of symmetry operations:   4
 Number of atoms in the asymmetric unit:  16
 Inversion center at the origin:   1

 Lattice parameters:   20.4040   3.8060  11.9080   90.000  120.236   90.000

 Symmetry operations

      0.000000 1 0     0.000000 2 0     0.000000 3 0
      0.000000-1 0     0.000000 2 0     0.000000-3 0
      0.500000 1 0     0.500000 2 0     0.000000 3 0
      0.500000-1 0     0.500000 2 0     0.000000-3 0

 Required memory size:    81    15    47    242544 (10000000)

 Potentials of sites in the asymmetric unit

          Charge      W        x        y        z          phi
 Ti1      4.626000 0.500000 0.078600 0.000000 0.636800 -3.146038E+00
 Ti2      4.285000 0.500000 0.293100 0.000000 0.367600 -3.096065E+00
 Ti3      4.714000 0.500000 0.888900 0.000000 0.630700 -3.404905E+00
 Ti4      4.846000 0.250000 0.000000 0.000000 0.000000 -3.901132E+00
 Ti5      4.769000 0.500000 0.185600 0.000000 0.006000 -3.570250E+00
 O1      -2.000000 0.500000 0.173800 0.000000 0.585900  2.122348E+00
 O2      -2.000000 0.500000 0.373000 0.000000 0.580000  1.942589E+00
 O3      -2.000000 0.500000 0.596700 0.000000 0.621000  2.093214E+00
 O4      -2.000000 0.500000 0.790900 0.000000 0.618800  1.798789E+00
 O5      -2.000000 0.500000 0.250800 0.000000 0.197300  1.814775E+00
 O6      -2.000000 0.500000 0.709400 0.000000 0.002200  1.868050E+00
 O7      -2.000000 0.500000 0.899600 0.000000 0.986300  1.609885E+00
 O8      -2.000000 0.500000 0.025000 0.000000 0.418800  2.043713E+00
 O9      -2.000000 0.500000 0.875300 0.000000 0.188500  1.795513E+00
 O10     -2.000000 0.250000 0.500000 0.000000 0.000000  1.458112E+00
 O11     -2.000000 0.500000 0.049500 0.000000 0.197900  1.636142E+00


 Electrostatic energy per asymmetric unit
    -27.314512 e**2/Å = -393.31946 eV = -37.949550 MJ/mol
```

5Cu-TiNb2O7 (Dreele)_refined

Oxygen Occ. = 0.993

```
*******************************
*   MADEL written by K. Kato  *
*   and modified by F. Izumi  *
*   v1.31, July 23, 2013      *
*******************************

 Ti Nb2 O7
 Radius of an ionic sphere:  1.30 Å
 Reciprocal-space range:  4.00 Å**(-1)
 Number of symmetry operations:   4
 Number of atoms in the asymmetric unit:  16
 Inversion center at the origin:   1

 Lattice parameters:   20.4040   3.8060  11.9080   90.000  120.236   90.000

 Symmetry operations

      0.000000 1 0     0.000000 2 0     0.000000 3 0
      0.000000-1 0     0.000000 2 0     0.000000-3 0
      0.500000 1 0     0.500000 2 0     0.000000 3 0
      0.500000-1 0     0.500000 2 0     0.000000-3 0

 Required memory size:    81    15    47    242544 (10000000)

 Potentials of sites in the asymmetric unit

          Charge      W        x        y        z          phi
 Ti1      4.626000 0.500000 0.078600 0.000000 0.636800 -3.145827E+00
 Ti2      4.285000 0.500000 0.293100 0.000000 0.367600 -3.095387E+00
 Ti3      4.714000 0.500000 0.888900 0.000000 0.630700 -3.405783E+00
 Ti4      4.846000 0.250000 0.000000 0.000000 0.000000 -3.905139E+00
 Ti5      4.769000 0.500000 0.185600 0.000000 0.006000 -3.571603E+00
 O1      -1.986000 0.500000 0.173800 0.000000 0.585900  2.111249E+00
 O2      -1.986000 0.500000 0.373000 0.000000 0.580000  1.930217E+00
 O3      -1.986000 0.500000 0.596700 0.000000 0.621000  2.081600E+00
 O4      -1.986000 0.500000 0.790900 0.000000 0.618800  1.785272E+00
 O5      -1.986000 0.500000 0.250800 0.000000 0.197300  1.800997E+00
 O6      -1.986000 0.500000 0.709400 0.000000 0.002200  1.854669E+00
 O7      -1.986000 0.500000 0.899600 0.000000 0.986300  1.593315E+00
 O8      -1.986000 0.500000 0.025000 0.000000 0.418800  2.031212E+00
 O9      -1.986000 0.500000 0.875300 0.000000 0.188500  1.781273E+00
 O10     -1.986000 0.250000 0.500000 0.000000 0.000000  1.441018E+00
 O11     -1.986000 0.500000 0.049500 0.000000 0.197900  1.619375E+00


 Electrostatic energy per asymmetric unit
    -27.178839 e**2/Å = -391.36582 eV = -37.761052 MJ/mol
```

Manawan, M., et.al. (2022) unpublished work

# Anisotropy Displacement Parameters

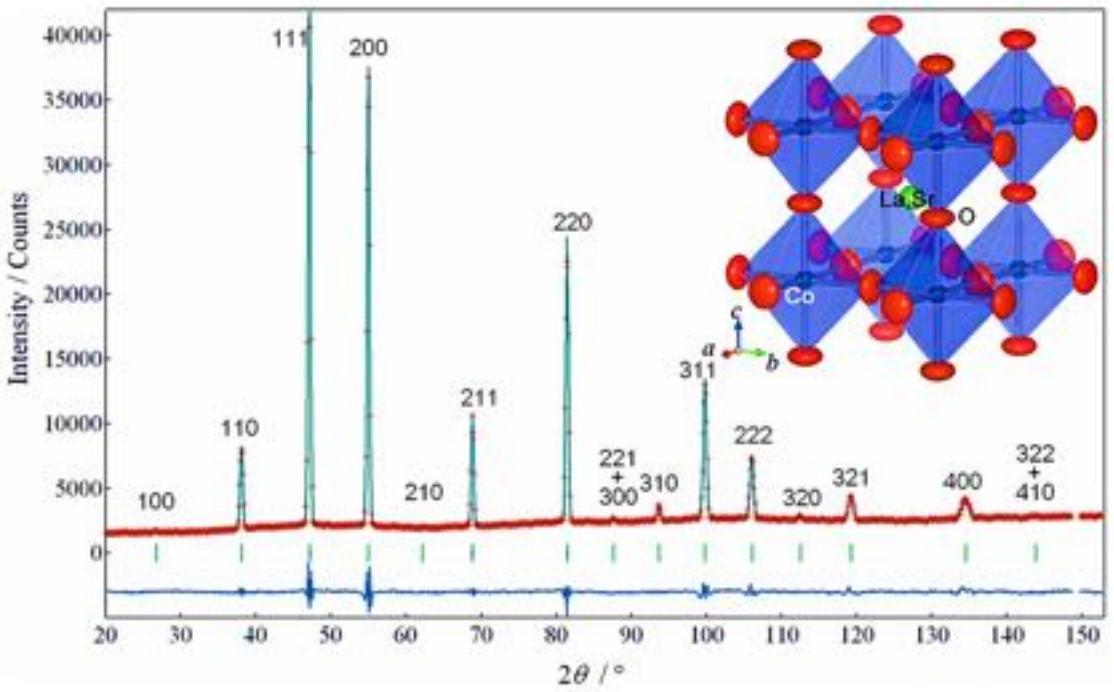


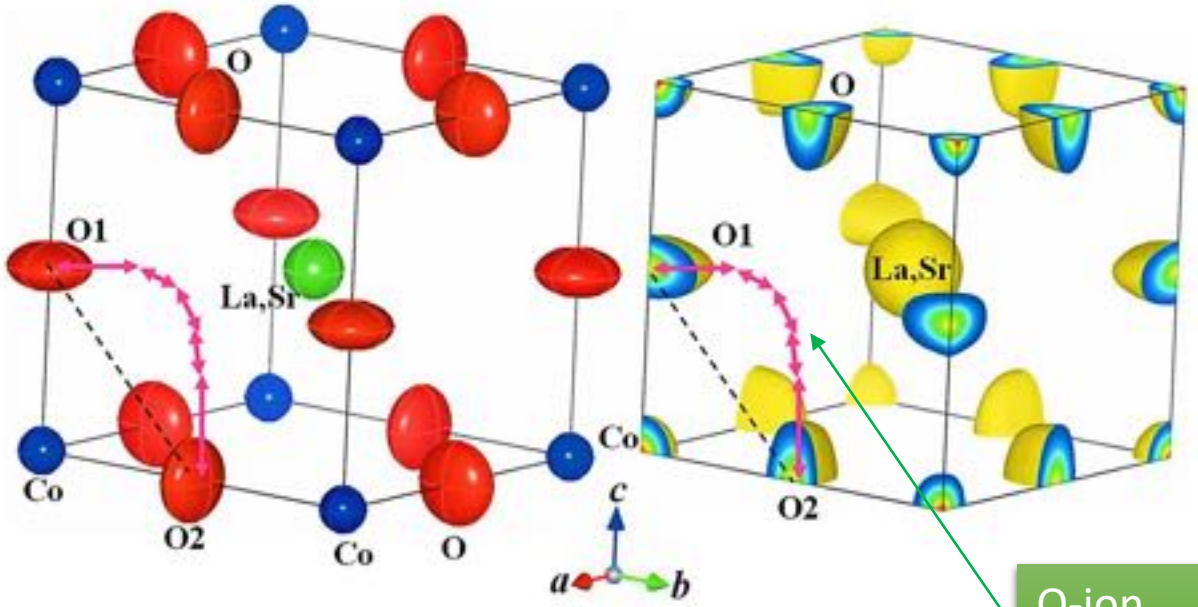


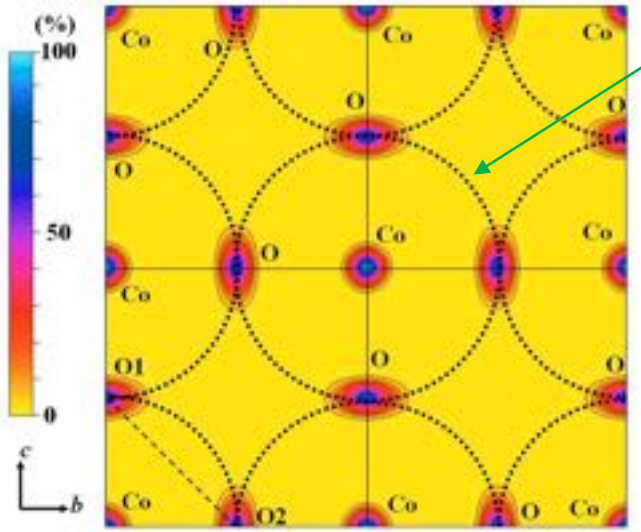


O-ion pathway

The crystal structure of a cubic $Pm\bar{3}m$ perovskite-type doped lanthanum cobaltite, $La_{0.6}Sr_{0.4}CoO_{3-\delta}$, has been studied using *in situ* neutron powder diffraction data measured at 1531 K. The refined occupancy 0.886 (6) of O atoms at the 3*d* 1/2, 0, 0 site indicated an oxygen deficiency of $\delta = 0.34$ (2) and an average valence of +2.7 for Co cations in $La_{0.6}Sr_{0.4}CoO_{3-\delta}$ at 1531 K. Refined anisotropic atomic displacement parameters and nuclear density mapping reveal that the oxygen ions in $La_{0.6}Sr_{0.4}CoO_{3-\delta}$ exhibit a large thermal motion perpendicular to the Co—O bond. A curved path for oxygen-ion migration between adjacent anion sites in $La_{0.6}Sr_{0.4}CoO_{3-\delta}$ is proposed, although it was not observed as a connected density in the experimental mapping.

M. Yashima, T. Tsuji, (2007) J. Appl. Crystallogr. 40, 1166

# Bond Valence and MaxEnt Method

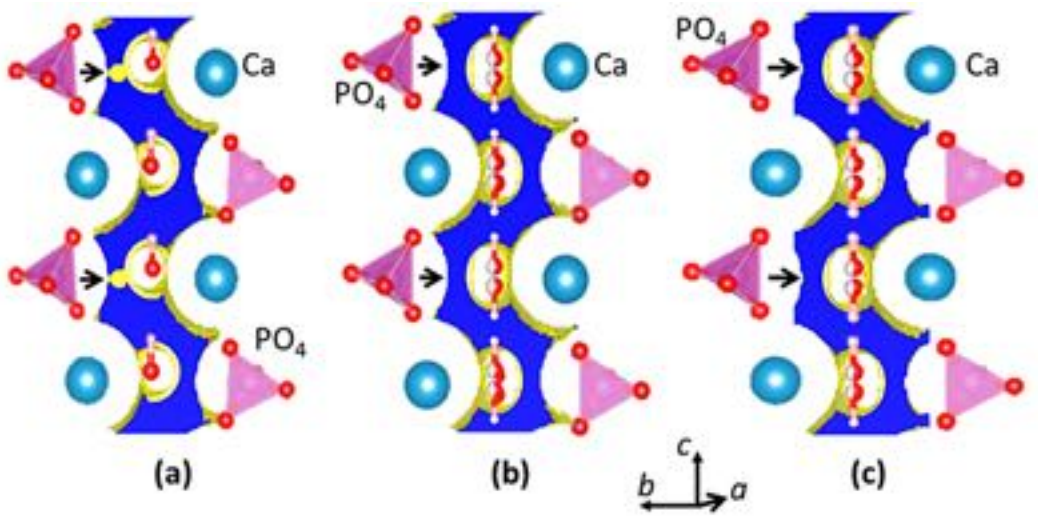


**Figure 9.** Refined structure with equi-density surface of difference bond valence sum (DBVS) at ±0.2 v. u. at (a) 298, (b) 673, and (c) 923 K. Arrows indicate the bottleneck for the proton diffusion. Red,

M. Yashima et.al. (2014) J. Phys. Chem. C 118, 5180

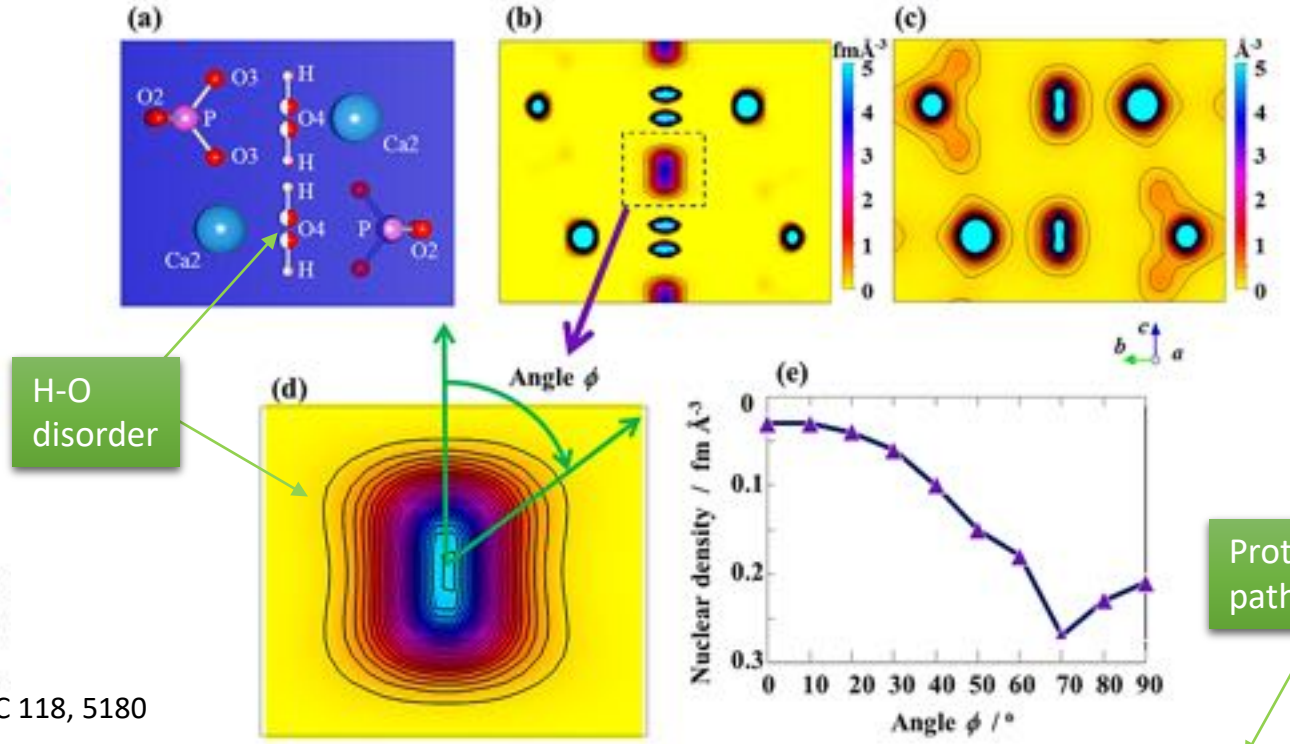


Proton pathway

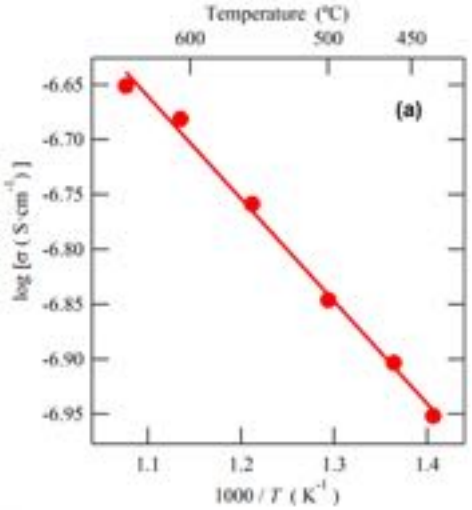


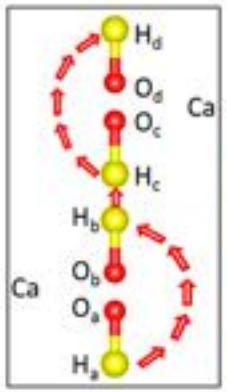


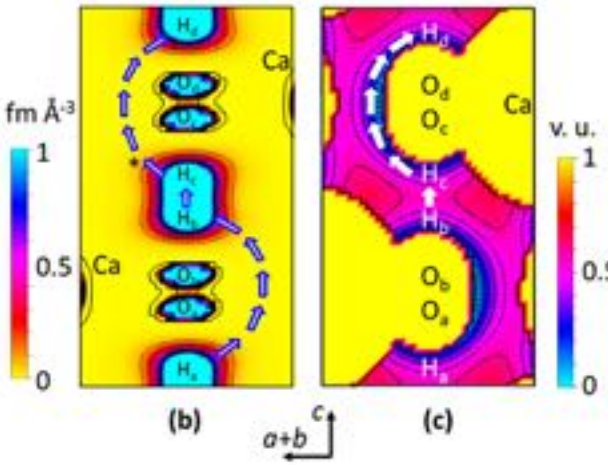


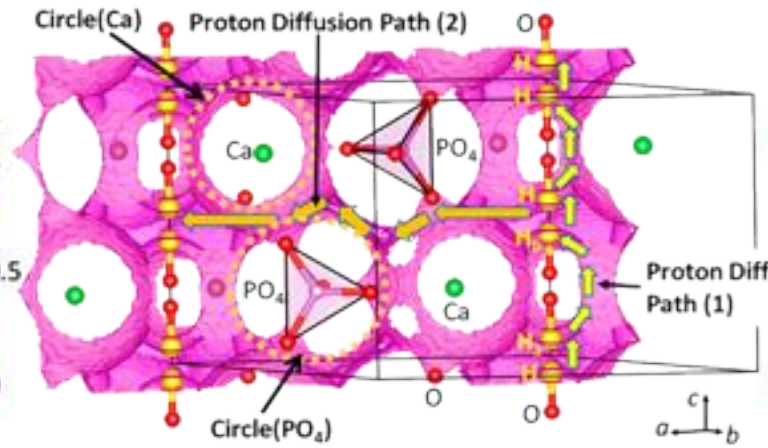


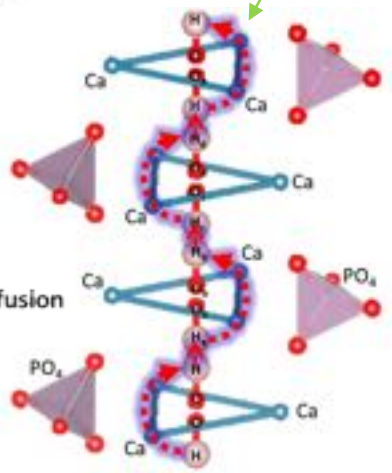

# Where is the Hydrogen ?

Disaccharide ($C_{12}H_{22}O_{11}$) molecule in sugar crystal structure

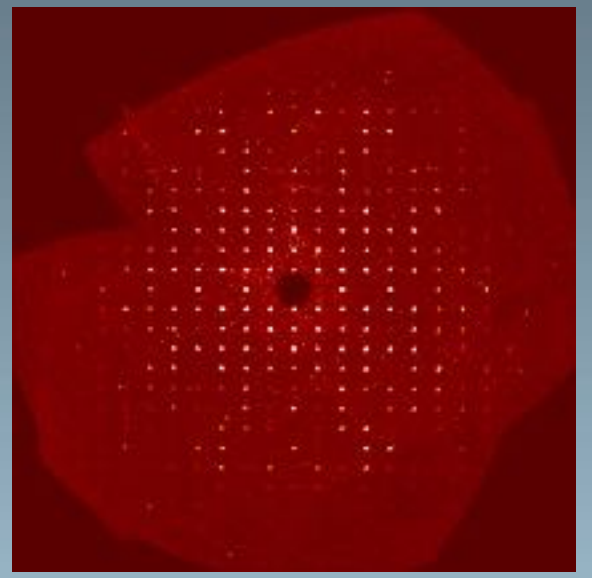

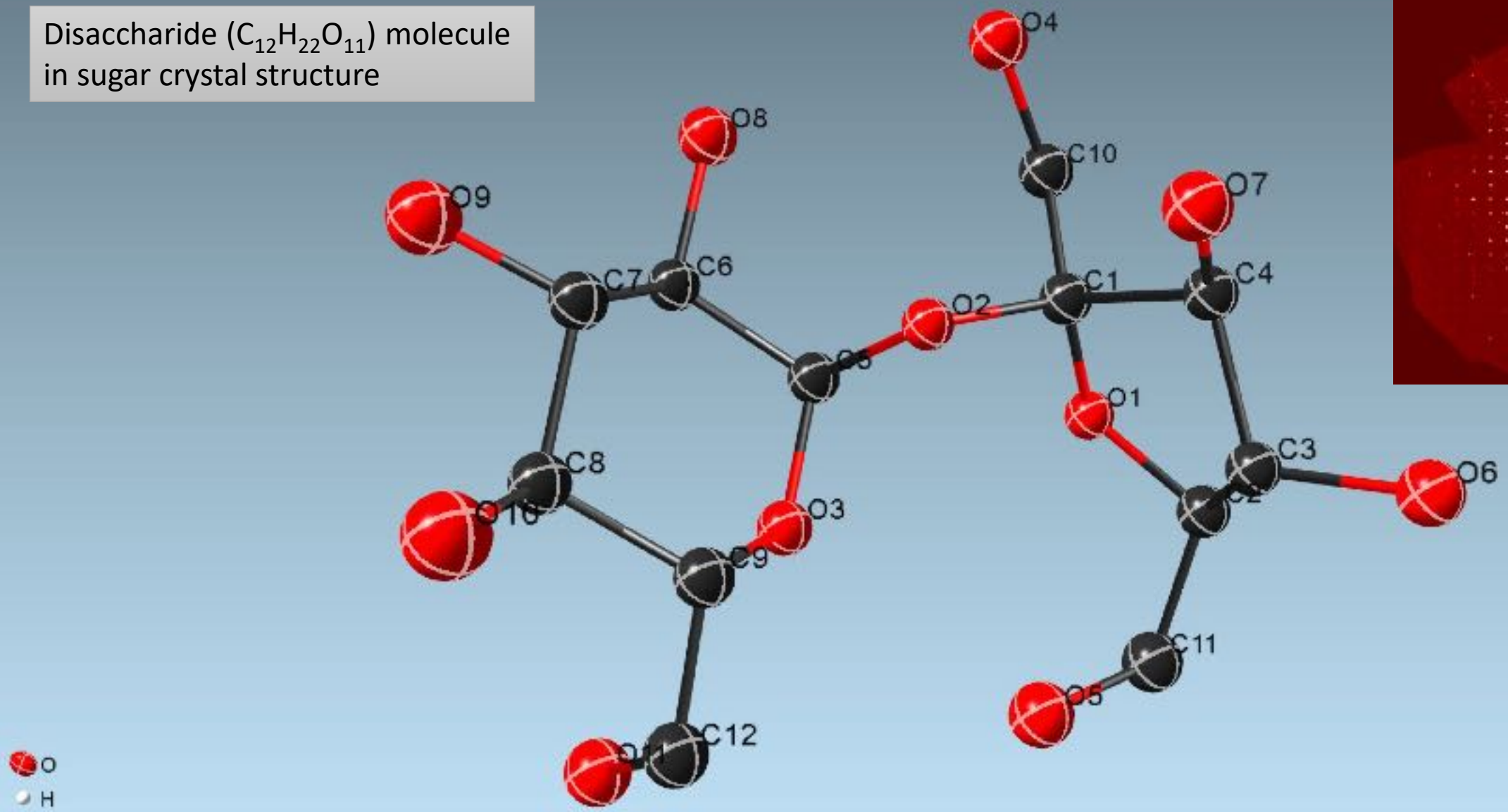

# Hole Doped Superconductor

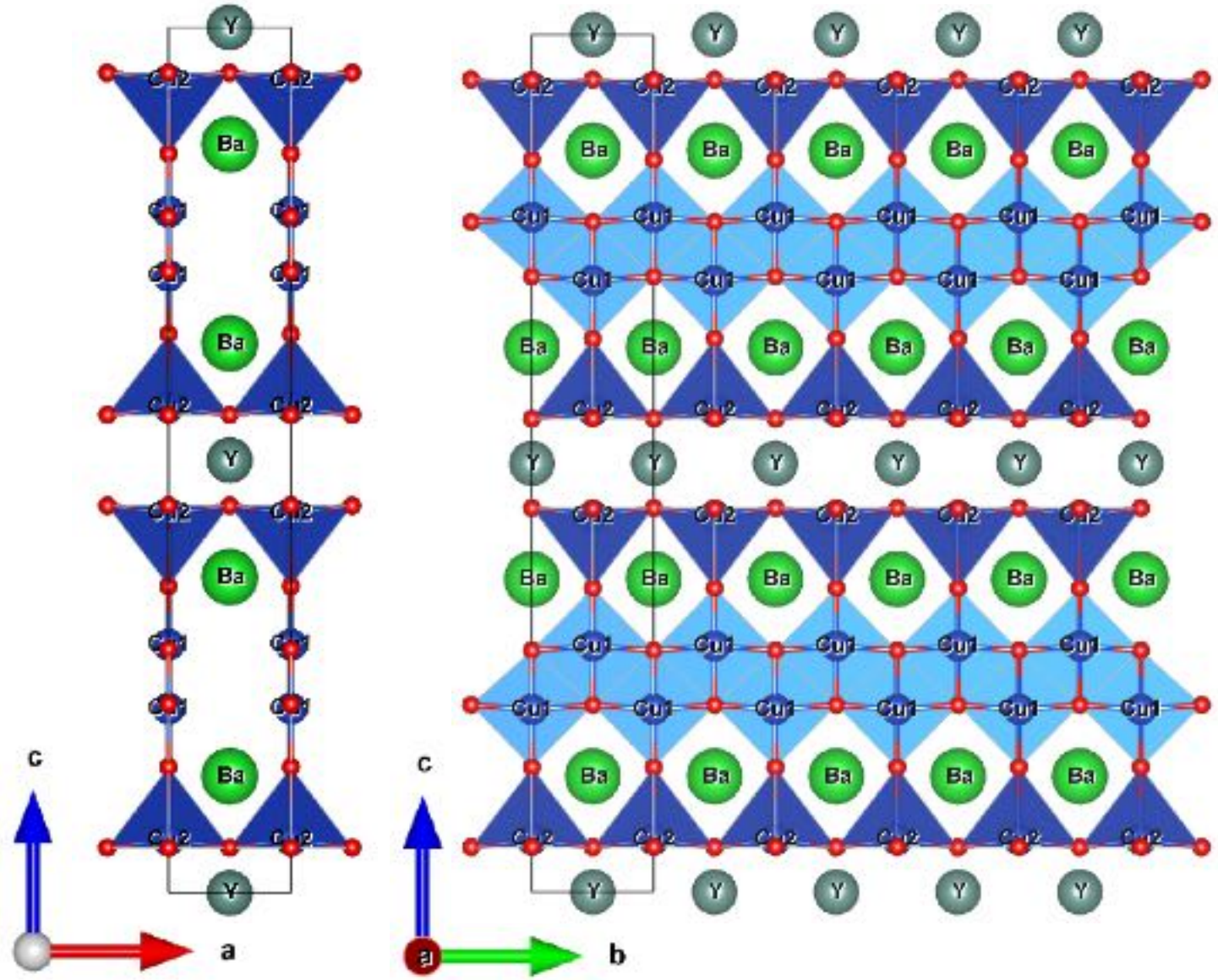


```
*********************************
 *   MADEL written by K. Kato    *
 *   and modified by F. Izumi    *
 *   v1.31, July 23, 2013        *
 *********************************

 Ba2 Cu4 Y O8
 Radius of an ionic sphere:  1.60 Å
 Reciprocal-space range:  4.00 Å**(-1)
 Number of symmetry operations:   8
 Number of atoms in the asymmetric unit:   8
 Inversion center at the origin:   1

 Lattice parameters: 3.8402 3.8708 27.2309 90.000 90.000 90.000


 Potentials of sites in the asymmetric unit

          Charge      W         x         y         z          phi
 Y         3.000000 0.125000 0.500000 0.500000 0.000000  -1.639969E+00
 Ba        2.000000 0.250000 0.500000 0.500000 0.135000  -1.330300E+00
 Cu1       2.000000 0.250000 0.000000 0.000000 0.213000  -2.164419E+00
 Cu2       2.500000 0.250000 0.000000 0.000000 0.061400  -1.798495E+00
 O1       -2.000000 0.250000 0.000000 0.000000 0.145600   1.310970E+00
 O2       -2.000000 0.250000 0.500000 0.000000 0.052500   1.931013E+00
 O3       -2.000000 0.250000 0.000000 0.500000 0.052100   1.925715E+00
 O4       -2.000000 0.250000 0.000000 0.500000 0.218200   1.133869E+00


 Electrostatic energy per asymmetric unit
     -3.318596 e**2/Å = -47.78662 eV =  -4.610707 MJ/mol
```

In the above calculation, all the holes are assumed to be doped into the Cu2 atoms on the CuO2 conduction sheet with the Cu1 atoms having an oxidation state of +2.

Izumi, F. (1991) Phys. C. 190, 35

# Fourier, MEM & BVS Software

- Fourier Synthesis
  - GSAS I (https://subversion.xray.aps.anl.gov/trac/EXPGUI)
  - GSAS II (https://subversion.xray.aps.anl.gov/trac/pyGSAS)
  - PROFEX (https://www.profex-xrd.org/)
  - FULLPROF (https://www.ill.eu/sites/fullprof/index.html)
  - JANA2006 (http://jana.fzu.cz/)

- Maximum Entropy Method (MEM)
  - Z-RIETVELD (https://z-code.kek.jp/zrg/)
  - RIETAN-FP (http://fujioizumi.verse.jp/download/download.html)
  - BayMEM (https://www.crystal.uni-bayreuth.de/en/baymem/index.html)

- Bond Valence Sum (BVS)
  - PyAbstantia* (https://shinichinishimura.github.io/pyabst/)
  - 3DBVSMAPPER** (https://www.ansto.gov.au/people/mr-matthew-sale)
  - VESTA (https://jp-minerals.org/vesta/en/download.html)

Note: *LINUX environment, **need Material Studio

# Professional Community & Collaborators

https://www.researchgate.net/profile/Maykel_Manawan

Maykel Manawan

Dr · Lecturer at Universitas Pertahanan Indonesia

Research Interest Score: **316.1** +1.30

99 *Crystallography, X-ray/Neutron Diffraction*

ICDD

Education Subcommittee

Introduction

Maykel Manawan currently works as a lecturer and researcher at Indonesia Defense University. An active member of the International Center for Diffraction Data, ICDD (Education sub-committee). Principal Investigator of the National Li-ion Battery Program (Battery Research Institute-Consortium). Member of Material Research Society Indonesia, MRS-INA. Member of Indonesian Magnetic Society. Member of Indonesia Neutron Scattering Society.

Skills and Expertise

Crystallography | Powder Diffraction | Neutron Diffraction | Protein X-ray Crystallography | Lithium Ion Batteries | Superconductivity and Superconduct... | Magnetic Materials and Magnetism | Density Functional Theory | Material Characterization | Ancient History

https://growkudos.com/projects/crystallography-and-diffraction


| | | |
|---|---|---|
| Email | : | maykeltem@gmail.com |
| Mobile (WA only) | : | +62 0812 1866 7095 |
| SCOPUS ID | : | 57202359553 |
| Web of Science ID | : | O-8852-2018 |
| ORCHID ID | : | 0000-0003-3782-1307 |
| Google Scholar | : | R6tOeqMAAAAJ&hl |
| SINTA ID | : | 6193883 |


SCIENCE
IT'S LIKE
MAGIC
BUT REAL


KNOWLEDGE
ANALYZE
DATA
FACT
RESEARCH
PRACTICE
100 %
SUPPORT
TESTING
DEVELOPMENT


STRATEGY
IDEAS
SOLUTION
PLAN
TEAMWORK

# THANK YOU